Abstract

Parkinson's Disease is a debilitating neuro-degenerative disorder which has a major impact on patients and their quality of life. The main pathological feature is the loss of dopaminergic neurons in the Basal Ganglia. Action selection and response inhibition two functions of the BG and also affected over the course of disease progression. It is possible to quantify response inhibition via the use of the Stop Signal Test, where PD patients show significant differences when compared to age matched controls. The goal of this paper is to create a model of the BG capable of simulating the Stop Signal Test. The model included several populations of the BG modelled as a set of spiking Izhikevic neurons with connectivity between populations. The Reaction Times and Stop Signal Reaction Times were compared between a normal and parkinsonian condition. The results indicate that there is a significant difference between the RT of the two conditions, $262.8ms$ vs. $274.8ms$, $p = 0.04$. There was no significant difference between the SSRTs of two conditions.

Simulation of the Stop Signal Test in a Basal Ganglia Model

Thomas Keizers

May 20, 2023

Contents

1 Introduction

1.1 Parkinson's Disease

Parkinson's Disease (PD) is a neurodegenerative movement disorder. It is the second most prevalent age related neurodegenerative disorder after Alzheimer's disease. It is estimated that 1% of the population over the age of 60 years old suffers from the disorder, rising to 3% in people over the age of 80 [4]. The common symptoms of PD are resting tremor, rigidity, bradykinesia and postural instability [17]. These symptoms are often referred to together as parkinsonism, which is a defining characteristic of PD. There are other disorders which feature parkinsonism, typically referred to as atypical Parkinson's Disorders, the most notable ones being; multiple system atrophy, dementia with Lewy bodies, progressive supranuclear palsy and corticobasal degeneration [40].

In addition to the movement symptoms, there are a slew of other non-movement related symptoms, which can greatly affect the patient's quality of life. Failure of the autonomic system is a common feature of PD, with patients experiencing among others orthostatic hypotension, sweating dysfunction, sphincter dysfunction and erectile dysfunction [17]. In addition to this, decline of cognitive faculties is also highly prevalent. In a follow-up study, it was found that 28.9% of PD patients developed mild cognitive impairment after a period of five years. The yearly prevalence of dementia development was also markedly increased compared to non-PD patients, PD-patients are four to six times more likely to develop dementia. 10% of PD patients develop dementia every year with a life-long prevalence of up to 80% [9]. Other neurological comorbidities include depression, anxiety and apathy [17].

The main focus for this thesis will be the inhibitory control system in the context of Parkinson's Disease. Response control is affected in PD due to it's relation

with dopamine and the dopaminergic medications commonly prescribed in PD can negatively impact this system, resulting in Impulse Control Disorders in some patients [21][5].

One method to quantify the effectiveness of the inhibition control system is through the Go/Stop test, which was first developed and mathematically formulated by Logan, Cowan and Davis in 1984 [19]. This experiment allows for the quantification of the reaction time to a stimulus as well as the reaction time to a stop stimulus, which can only be determined indirectly. It is assumed that the time to inhibit a response is shorter than the reaction time. This seems to be sound as otherwise inhibition of an ongoing action would be impossible.

In the Stop Signal Task test subjects are asked react as quickly as they can to a presented stimulus, a signal called the Go cue. Commonly, subjects will be situated in front of a computer screen which will display a visual indicator. As soon as this indicator appears, the subjects should respond. In most cases the subjects will have to press a button, which will register the Go Reaction Time (GoRT). After a reaction has been given the indicator will be removed from the screen. In between cues, separate mark is present on the screen to allow subjects to more easily focus on the centre of the screen.

A certain percentage of trials will be Stop Trials instead, usually 25% of the total number of trials to reduce anticipation effects. A Stop Trial will start the same way as a Go Trial. However, after the Go cue has been presented, following a fixed delay, a Stop cue will be given to the subject. This delay is dubbed the Stop Delay (SD) and is usually in the order of a 100 ms. The subjects have been instructed that in the case of this second signal, they should attempt to refrain from pressing the button. Additionally, it is emphasized during the briefing that it is not always possible to abort the button press and that the reaction speed is more important than accuracy. The Stop Trials where subjects successfully inhibit their response are dubbed successful stops, and the trials were they were unable to stop themselves are called failed stops. The failed stops will yield a GoRT as the action has not been inhibited.

A full course of testing consists of multiple blocks of trials divided by periods of rest, to prevent fatigue. The first block of the course will consist of only Go Trials, in order to obtain the distribution of the GoRTs for a particular subject, as well as to allow the subject to train and familiarize themselves with the experiment. After this initial training phase, Stop Trials will be randomly mixed into the blocks in the aforementioned ratio. In Figure 1 an example of a series of trials is shown. Here the subjects are given multiple options in response to a Go Cue and the Stop Cue is auditory. This image was first published in Verbruggen et al. [38]. The data obtained from these testing blocks will be used to calculated the inhibition success rate as a function of the Stop Delay.

The SD is dynamically altered over the course of the trial in an attempt to obtain an approximately 50% success rate of inhibition. Every successful Stop Trial will increase the SD, giving subjects less time to inhibit their response.

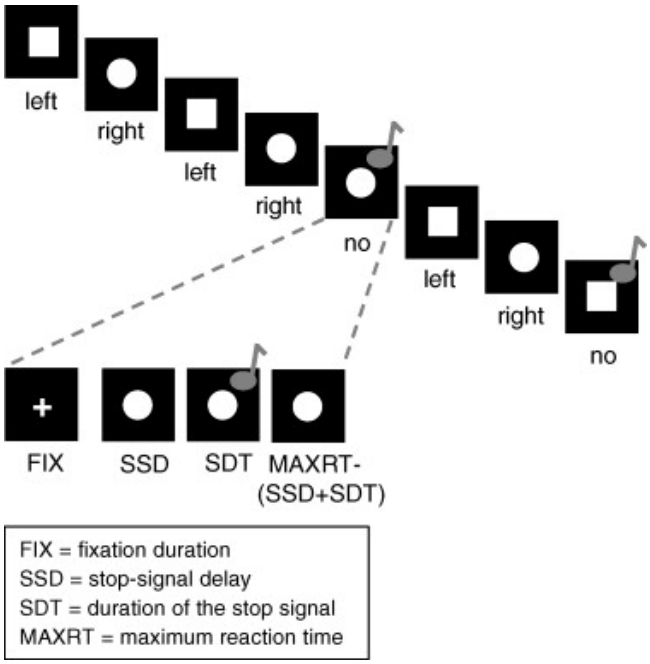

Figure 1: This figure presents an example of a Stop Signal Task block with Stop Trials interspersed between Go Trials. In this example subjects are given two different Go stimuli which should elicit two different responses, a left button for a square image and a right button for a circle image. The Stop Cue takes the form of a sound which informs the subjects to inhibit their response. The fixation duration is the time that the fixation mark is presented to the subject, after which the Go Cue is presented. The SSD corresponds to the Stop Delay. The SDT is the period during which the Stop Signal is continously presented. The MAXRT is the maximum time allotted for a reaction to be given. If a response is given within this period a GoRT will be registered. If no response is given, this will be registered as a successful inhibition. Image originally published in Verbruggen et al. [38]

Every failed Stop Trial will decrease the SD, allowing subjects more time to respond. After a sufficient number of trials has been performed, the average SD will correspond to a 50-50 inhibition success rate.

The Stop Signal Reaction Time (SSRT) can be calculated from two test parameters obtained from this course of experiments. The first parameter is the distribution of GoRTs, which are obtained from the initial testing block. The second is the SD for which the success rate of inhibition is 50%. The SSRT can then be calculated by subtracting the SD from the average GoRT. In Figure 2 the relation between the distribution of the GoRT and the SD are made more apparent, this figure was originally published in Wang et al. [39]. Reaching a success rate of inhibition of 50% is the goal over the course testing, because this eases the determination of the SSRT.

The relevance of the Stop Signal Test was demonstrated by Gauggel, Rieger and Feghoff [7]. Following findings that lesions in the basal ganglia correspond

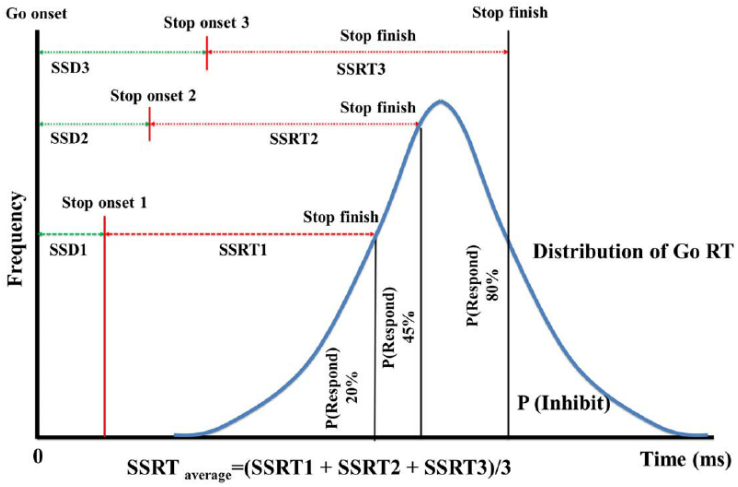

Figure 2: The blue curve displays the probability distribution of the Go Reaction Times following a Go cue. The Stop Finish line marks the point in time at which a stop process has finished. The area under the curve to the left of this line gives the probability that an action will occur in spite of a stop signal. The area under the curve to the right of the line is the chance of successful inhibition. Finding the relationship between the Stop Delay and the probability of inhibition will allow one to calculate the cumulative probability distribution of successful inhibition. The difference between the Stop Delay value which yields 50% inhibition success rate and the average GoRT is the Stop Signal Reaction Time. Image originally published in Wang et al. [39]

to deficits in inhibition, they compared PD patients with an age matched control. They found that PD patients had significantly longer SSRTs, even when compensating for general differences in reaction time between groups. These findings show the relevance of the Stop Signal Test for PD as a potential quantifier and a method to show the efficacy of PD treatments, which can be used as an additional parameter alongside e.g. the Hoehn and Yahr scale.

1.2 Basal Ganglia

The role of the basal ganglia (BG) in movement control is primarily that of a controller. It takes input from the cortical regions, which arrives in the striatum. The output target is the thalamus. Depending on the input the thalamus can be inhibited, disallowing it from relaying movement related signals, or alternatively disinhibited, promoting its relay function.

The primary pathological feature of PD is the degeneration of dopaminergic neurons in the substantia nigra pars compacta (SNpc). This phenomenon eventually leads to depletion of dopamine (DA) levels throughout the brain, but especially in the striatum [3]. The striatum is an important part of the BG, playing an integral role in the regulation of movement. The decreased presence of DA in the striatum affects functionality of the Medium Spiny Neurons (MSN),

which are responsible for the relay of signals downstream to the globus pallidus and represent the majority of striatal neurons. This pathological development in the BG is considered to be the main driver of the movement symptoms of PD. Specifically, the decreased activation of DA receptors affects the synaptic surface expression of AMPA receptors. These receptors are responsible for excitation in response to glutamatergic signals from the cortex. D1-type receptor activation increases the surface expression of AMPA receptors and D2-type receptor activation decreases the surface expression of AMPA receptors, among other effects. The lower ambient levels of DA present in PD, thus has a inhibitory effect on D1-type expressing MSNs and a excitatory effect on D2-type expressing MSNs [34].

The vast majority of the neuronal connections within the BG are inhibitory in nature. This inhibition is facilitated through release of the neurotransmitter γ-aminobutyric acid (GABA). GABA activates the GABA-receptors in the cell membrane of the post-synaptic neuron, which leads to a transient flux of Cl^- ions into the cell. This causes temporary hyperpolarization, decreasing the likelihood of an action potential being generated. A relatively small portion of the neuronal connections within the BG are excitatory. Excitation is facilitated through the release of the neurotransmitter glutamate, which binds to the AMPA receptors present on the cell membrane. Activation of the AMPA-receptors sets in motion a transient flux of Na^+ and K^+ ions, depolarizing the membrane and increasing the likelihood of an action potential being generated. Both types of receptors are present on the cell membranes of all neurons within the BG. The sensitivity of a certain neuron to a specific neurotransmitter is a function of the amount of receptors present on the membrane. The nature of the pre-synaptic neuron is the determining factor for which neurotransmitter gets released in response to an action potential arriving at the synapse. The sensitivity of the post-synapse to the neurotransmitter of the pre-synapse, as well as the amount of neurotransmitter released, determines the connectivity strength between any two neurons.

The signal processing pathways and the effects can be explained in terms of a direct and indirect pathway. The cortical input for action selection arrives at the striatum. There exist two different populations of MSNs which either primarily express D1 dopamine receptors or D2 dopamine receptors. These two populations project to different parts of the globus pallidus, which form the basis for the direct and indirect pathways. The D1 expressing MSNs project inhibitory signals to the Globus Pallidus Interna (GPi), which disinhibits the thalamus. The D2 expressing MSNs project inhibitory signals to the Globus Pallidus Externa (GPe). The GPe forms a neural circuit with the Subthalamic Nucleus (STN), where the GPe inhibits STN activity and the STN has excitatory projections to the GPe in addition to sending excitatory signals to the GPi. In this simplified framework the direct pathway promotes thalamic signal relaying and the indirect pathway inhibits thalamic activity [34].

In addition to the pathways of the classical BG model, another site of corti-

cal input in the STN has been suggested to form a hyperdirect pathway [24]. The shorter transmission delays of the cortico-subthalamic connection and the overall shorter length of the pathway to the thalamus allows the hyperdirect pathway to influence the thalamus before the other signals arrive. The excitation of the STN sends excitatory signals to the GPi, which would inhibit thalamic activity. The three pathways together are suggested to function as a dynamic 'center-surround model'. The hyperdirect pathway broadly inhibits the thalamus around a certain desired motor programme. The direct pathway disinhibits the specific motor programme to be executed. Finally, the indirect pathway would inhibit the motor programme ending this instance of motor activity. This process would ensure that only a single action is allowed to be enacted from a list of competing actions involving the same motor outputs, preventing simultaneous activation. An example of this model using simple spiking data can be seen in Figure 3 from the work by Hashemiyoon et al. [12]. A comparison between the 'classical' model, consisting of solely a direct and indirect pathway, and a more contemporary model can be seen in Figure 4, as originally seen in a paper by Simonyan [33].

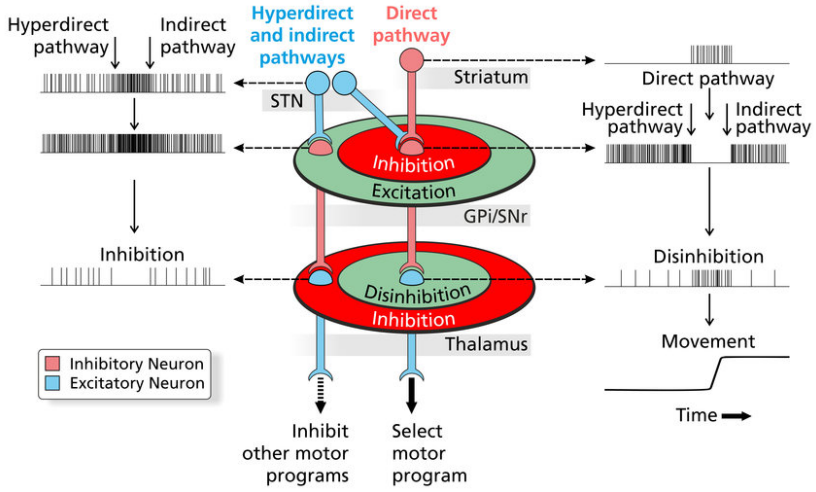

Figure 3: A representation of the dynamic behaviour of a centre surround model is depicted here in terms of simple spiking neurons. Initially, the hyperdirect pathway broadly excites a portion of the STN, which projects onto the GPi/SNr, leading to diffuse thalamic inhibition. This is followed by specific inhibition of the GPi/SNr via the direct pathway, enabling disinhibition of only a specific portion of the Thalamus, whilst surrounding thalamic neurons remain surpressed. Finally, disinhibition of the STN via the indirect pathway once again causes diffuse excitation of the GPi/SNr inhibiting the thalamic relay neurons. This brief window of disinhibition of the select ghalamus neuron is what allows for the motor function signal to be passed along. Image originally published in Hashemiyoon et al. [12].

The BG receive a constant stream of sensorimotor and associative input from the cortical areas upstream. To facilitate in the execution of multiple programmes simultaneously and aid in task switching, a certain degree of parallel processing

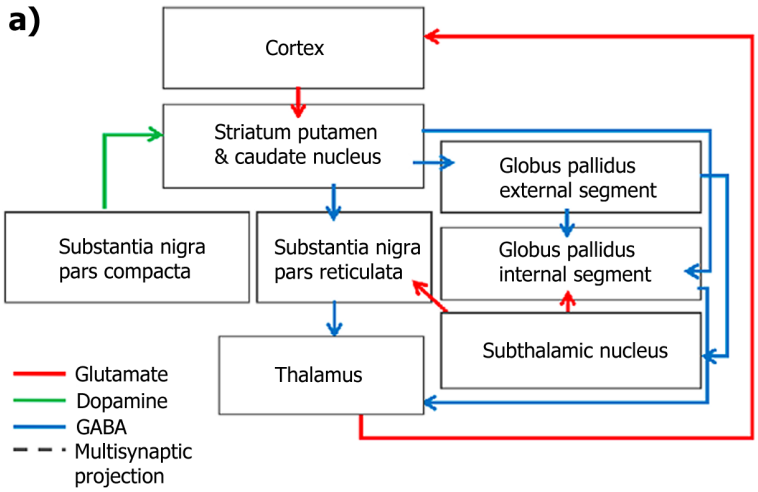

(a) Classical Model

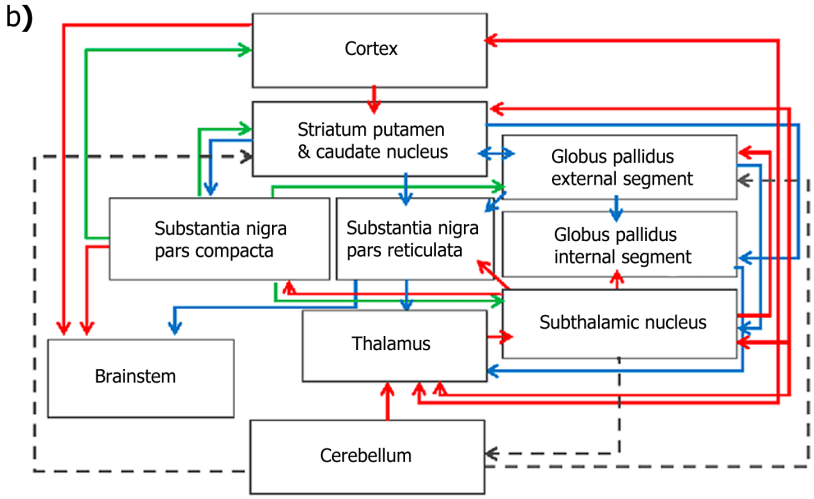

(b) Contemporary Model

Figure 4: a) The classical model of the basal ganglia as envisioned roughly 25 years prior. Note the relative self-containment of the basal ganglia, having only a single input and output site. The only form of internal feedback envisioned at the time was the STN-GPe loop. b) The contemporary model of the basal ganglia, the basal ganglia are more integrate with external circuits compared to what was presumed previously. A major cortical input site in the STN, corresponding with the hyper-direct pathway, has been described, with this current scheme allowing for dynamic action selection. The current model is markedly more complex in terms of connectivity between the various nodes, and new neuronal pathways have been discovered since, and will most likely by found in the future. Image originally published in Simonyan et al. [33].

within the BG has been proposed [18]. The presence of a clear bodymap topography being preserved within the multiple nuclei of the BG has been cited as evidence for the segregation of functional pathways. A certain degree of communication between these pathways would still be necessary in order to process only the most salient programmes. A detailed scheme for communications between paths has yet to be described. Tracer studies show a greater degree of convergence between striatonigral pathways in comparison to striatopallidal pathways [6]. This would suggest that interactions between functional pathways occurs in this domain. This is conform with the Centre Surround model and this framework would allow for action selection between multiple options.

The realization of the Centre Surround model in the BG can be described in terms of the hyperdirect model for multiple pathways. Initially broad inhibition of the thalamus is achieved via the diffuse excitation of the STN via the hyperdirect pathway. This cortical stimulation is non-specific and applied broadly to a portion of the STN. Next, the striatum will receive cortical input with pathway specific salience, which is passed along to the GPi. In the striatum the multiple pathways act simultaneously to inhibit their specific GPi parts as well as their neighbouring, parallel pathways. Once an action has been selected by the thalamus, the STN will once again receive broad excitatory input via the thalamocortical pathway which will halt further thalamic activity. At the same time the input into the striatum will be extinguished as well, preventing further action selection. This process will ensure only a single action is selected during this period while allowing for multiple inputs and functions to be processed simultaneously. A simplified scheme for this architecture can be seen in Figure 5.

1.3 Current Treatment Strategies

As of yet there exists no cure for Parkinson's Disease, and thus the treatment of the disease has been focused primarily on alleviation of the symptoms. The two primary therapies are medication and surgical intervention. Early treatment often utilizes medication to reduce symptoms and as the disease progresses and medication alone is no longer enough, clinicians and patients may opt for surgical intervention.

1.3.1 Pharmacological therapies

After the discovery in 1960 that a major driver of the PD pathology was dopamine deficiency, Levodopa was soon thereafter developed as a pharmaceutical treatment for the parkinsonian movement symptoms [13]. Levodopa is the precursor to dopamine and can cross through the blood brain barrier to arrive at the affected sites and alleviate the dopamine deficiency. Although Levodopa reduces motor symptoms and is currently still the primary treatment for PD, it has significant side effects. Up to 40% of patients experience motor fluctuations and up to one third of patients experience dyskinesias within 4 - 6 years of Levodopa use [23]. To help reduce the impact of these side effects, Levodopa is

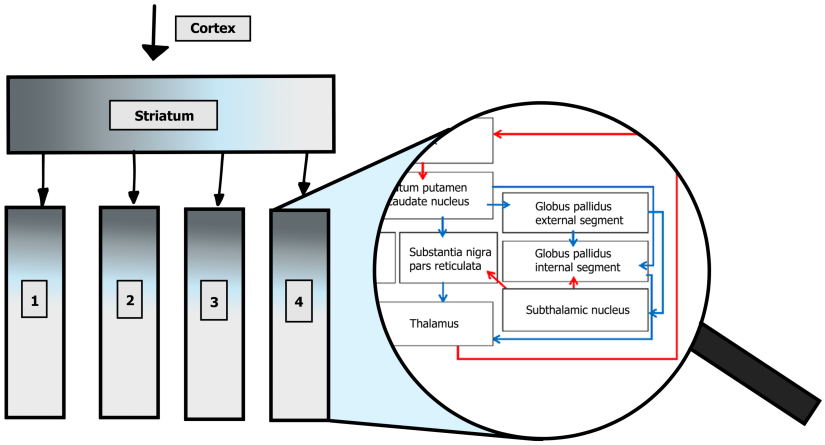

Figure 5: Functional segregation of the Basal Ganglia manifests via the topographical organization of the majority of subpopulations. Outside of the striatum, where lateral connections are abundant, the BG can be envisioned as consisting of parallel pathways for separate functions. These pathways have relatively few interconnections and in action selection compete to have their function executed. Through broad inhibition of these pathways via the diffuse excitation of the STN and pathway specific input through the striatum, as well as lateral inhibition between MSNs, the basal ganglia can function as a centre surround system. Each pathway independently contains all the nodes present in the contemporary model, minus the shared striatum.

frequently combined with additional medication which reduces the conversion rate of Levodopa, increasing the period of bioavailability and smoothing the concentration curve.

Another class of medication prescribed to combat the symptoms of PD are dopamine agonists. These interact with the dopamine receptors present in the striatum and increase the sensitivity to what little dopamine is present. These can be used as a monotherapy, or in combination with Levodopa. While the development of dyskinesia appears to be lesser in dopamine agonist therapies compared to Levodopa therapies, there is a higher prevalence of hallucinations [35]. Neither medication has been concluded to have any neuroprotective properties and serve only for combating symptoms.

The effects of pharmacological therapy does not seem to greatly impact the SSRTs of PD patients. In a 2015 paper Claassen et al. [2] compared the SSRT and related parameters between healthy control, PD patients with and PD patients without Impulse Control Disorder. Within either group of PD patients, there were those who received dopamine agonist monotherapy and those who received dopamine agonist and Levodopa co-therapy. It was shown that PD patients, regardless of therapy received, had significantly longer SSRTs than the healthy control group. Furthermore, whether the patients were ON or OFF dopamine agonists had no significant effect on the SSRT. The authors have noted, however, that the 24 hour washout period for medication might

not be comparable to full withdrawal. Additionally, the SSRT was found to be slightly faster in the group taking Levodopa compared to the dopamine agonist monotherapy group, but this difference was not statistically significant.

In addition to dopamine, noradrenaline, another neurotransmitter, has been implicated in the inhibitory pathways of the BG. Atomoxetine, a noradrenaline reuptake inhibitor, was tested in a double blind crossover study fMRI imaging study, which involved the stop signal paradigm [42]. Here it was not found to have a significant effect on the SSRT compared to placebo.

1.3.2 Surgical therapies

In the past two decades, in addition to pharmacological treatment, Deep Brain Stimulation (DBS) has been gaining traction as a method to treat PD [22]. DBS is a surgical intervention in which a device is implanted either unilaterally or bilaterally at the BG. The most common targets for stimulation are the STN or the GPi. Stimulation of either site is able to provide relief of symptoms and an increase in quality of life, with only small differences in side effects and power usage depending on the target. When patients receive diminishing returns from medication treatment, DBS may be considered and after a proper screening can be prescribed as an additional treatment method. The exact mechanism through which DBS reduces symptoms in PD is as of yet under investigation.

The influence of DBS on the SSRT in PD patients was studied early on, after the link between the BG and action inhibition was established. Van den Wildenberg et al. [37] studied the effect of STN-DBS and thalamus-DBS, in PD patients and patients with essential tremor, on motor response selection and response inhibition. Comparing the results of subjects on or off stimulation determined a significantly faster SSRT during the on-condition for patients with PD. Later on, Ray et al. [30] expanded upon this research by investigating the effect difference between unilateral stimulation of the right vs. the left STN. It was found that improvement of SSRTs during DBS primarily affected patients with significantly slower SSRTs off-stimulation. PD patients with SSRTs comparable to age-matched controls, did not experience a significant shortening of the SSRT.

1.4 Computational models of the Basal Ganglia

Neuroscientists have put together various models to help explain different parts of the neural circuitry, in spite of the immense complexity of the human brain. The BG are no exception to this push towards neurocomputational exploration. A model of particular relevance expanding the view of the BG as a central node in decision making is the action selection model by Gurney, Prescott and Redgrave [10]. In this article the authors lay the foundation for the BG as a central node capable of action selection, whether these actions be simple motor programmes or more complex cognitive behaviors. It is posited that the conventional 'direct' pathway could be described as the pathway through which the various actions race to be expressed and the 'indirect' pathway as the controller

which oversees the suppression of the actions which do not reach the requisite threshold for activation.

In the companion piece to the previous article the authors modeled their proposed architecture using leaky integrators as simplified neurons [11]. Using salience as a scalar input into the BG network, they found it possible to simulate signal selection. Furthermore, the influence of dopaminergic input was modeled phenomenologically. Low DA availability led to little to no action being selected even for normal salience, whereas high DA availability led to the selection of multiple tasks.

Another instance of BG modeling was performed by Rubin and Terman in 2004, establishing the eponymous Rubin-Terman model [31]. The goal of this model was to explain some seemingly paradoxical experimental results. It was indicated that in PD the output nuclei of the BG were overactive, preventing the thalamus from performing its relay function. Another observation is the reduction of PD symptoms through DBS therapy. Lastly there were experimental results indicating that particularly high frequency stimulation ameliorated symptoms by stimulating the STN which excited the BG output nuclei further. Rubin and Terman used their computational model to explain how the excitation of the GPi via DBS could improve thalamic relay functionality in the case of PD.

This model provides an architecture in which the STN-GPe loop and its connection to the GPi is described. With this model they were able to explain the seeming paradox between heightened activation of the GPi in PD being associated with motor symptoms, particularly tremor activity, and the excitation of the STN and GPi via DBS ameliorating these motor symptoms. It was shown in the simulations that the regularization of GPi firing patterns via DBS, despite being higher frequency than in the healthy situation, was able to preserve the thalamic relay activity.

This model established abnormal synchronization in BG subpopulations was a contributing factor in the pathological behaviour observed in PD. To this day, the STN-GPe loop is a major region of interest in neurocomputational models of the BG, especially after the discovery of the hyperdirect pathway by Nambu et al. [24], giving the STN even more importance.

A recent example of the use of computational models to investigate the effect of differing dopamine levels in the basal ganglia can be found in the paper by Navarro-López et al. [25]. Using a dynamic model they investigated the emergence of oscillatory behavior in the BG nuclei as a function of dopamine levels. The spectral power levels of different subpopulations of the BG were compared between cases of normal and parkisonian levels of dopamine within the striatum. Furthermore, action selection was modelled through the addition of a phasic dopamine component. The presence of a phasic DA component increases the influence of the direct pathway over the indirect pathway, causing the thalamus to act as a relay for cortical input. The thalamic response to

cortical input for both the presence and absence of a phasic DA component was compared between normal and Parkinsonian conditions as well.

In the simulations spectral power in the beta frequency range, commonly associated with PD, start to increase as the dopamine levels decrease. The beta frequency oscillations manifested as pervasive and synchronized spiking of neurons within BG nuclei at frequencies within the range of 13 to 30 Hz. However, this synchronized activity was not enough to interfere with the relay function of the thalamus by itself. Furthermore, for tremor activity to become observable in response to cortical input it was not enough to lower the dopamine levels. Tremor response only became apparant after the GPi-Thalamus connectivity was increased as well.

With the recent discovery of additional subpopulations within the GPe, new theories for the potential role they might play within action inhibition have been developed, dubbed the 'pause-then-cancel' model [32]. These subpopulations of the GPe have been dubbed the Prototypical GPe (GPe-Proto), the Arkypallidal GPe (GPe-Arky) and the Cortico-Pallidal loop GPe (GPe-CP). A theory put forward describes the activation of the STN via diffuse cortical activity as pausing the transmission of action signals to the thalamus. If the action was to be stopped, projections from the GPe-Arky can stop the action by projecting inhibition to the striatum to halt further transmission of an action signal. To test this theory Goenner et al.[8] developed a model which included the additional pathways within the GPe and simulated the Stop-Signal tests as performed by Mallet et al. [20]. Using populations of spiking Izhikevic neurons they were able to simulate the Stop-Signal task and investigate potential modes of failure of the model. After having succeeded in modeling Mallet's experimental data, obtained from Stop Signal tasks in rats, it was found that increased activity in the arkypallidal neurons corresponded more highly with Stop activity than general GPe neurons. This lead to the conclusion that the arkypallidal cells play a significant role in the inhibition of previously initiated actions.

This specific model by Goenner et al. will be referred to as the contemporary model from this point onward and is the basis for the model implemented in this paper. In Figure 4 the conception of the BG at the start of the 21st century can be seen alongside the contemporary model. This highlights the increase in complexity of the BG models as well as the advances in imaging studies, which allow for the discovery and tracing of new connections. This will only continue as time marches on.

1.5 Aim of the Research

The goal of this paper is to create a model of the BG which simulates the relevant nuclei with cellular interactions. The functional segregation of the BG will be modelled through the presence of parallel pathways, from the striatum onward, each having individual thalamic targets. This model will be used to simulate the Stop-Signal Test to determine whether or not the current description of the

architecture can adequately simulate the results for normal and parkinsonian conditions. The presence of parallel pathways will be tested and the influence this has on the outcomes of the Stop Signal Tests will be compared to the original model of Goenner et al.

2 Method

2.1 General Architecture

The BG are described as a collection of spiking Izhikevic neuron populations, the parameters of which are given below. The connectivity between and within these populations is based on the contemporary model as portrayed in Goenner et al. [8]. A similar connectivity scheme is followed in this model. There are three input nodes into the system, corresponding to cortical stimulation of the three pathways of the BG. Excitation of the D1- and D2-type Striatal neurons, which project to the GPi and GPe respectively, diffuse excitation of the STN, simulating cortical stimulation via the hyperdirect pathway, and cortical excitation of two specific subpopulations of the GPe, the GPe-Arky and the GPe-CP. All of these pathways converge onto the output nucleus, the thalamus, via the GPi. A schematic representation of the BG can be seen in Figure 6, originally depicted in Goenner et al. [8]. The model consists of four pathways existing in parallel with each other. Communication between these pathways is restricted to internal inhibition within the striatum. Go activity is determined on a per pathway basis. Separate integrators for the GO- and Stop-activity give the model outcome per trial.

2.2 Neuronal Model

The neurons in this model are described using the Izhikevic equations for spiking neurons [15]. The parameters for these neurons as are based on previously published work. The parameters for the striatal neurons, the D1-type MSNs, the D2-type MSNs and the Fast Spiking Interneurons (FSI), are based on the model of Humphries et al. [14] published in 2009. The STN and GPi parameters are based on the model of Thibeault and Srinivasa [36] published in 2013. The parameters for the thalamus are based on the set for a tonic spiking neuron by Izhikevic [16] in 2004. Finally the parameters for the different GPe subpopulations are based on the set given in Goenner et al. [8]. The synaptic weights for connections between neurons are based on the model by Goenner et al. [8] and the parameter set outlined above was used in this paper as well. Slight modifications to these parameters have been made to fit to the different architecture used in the model as well. These will be given in the section below. The differential equations governing the behaviour of the neurons are as follows:

$$\frac{dv}{dt} = n_2 v^2 + n_1 v + n_0 - \frac{u}{C * dt} - g_{AMPA}(v - E_{AMPA}) - g_{GABA}(v - E_{GABA}) \quad (1)$$

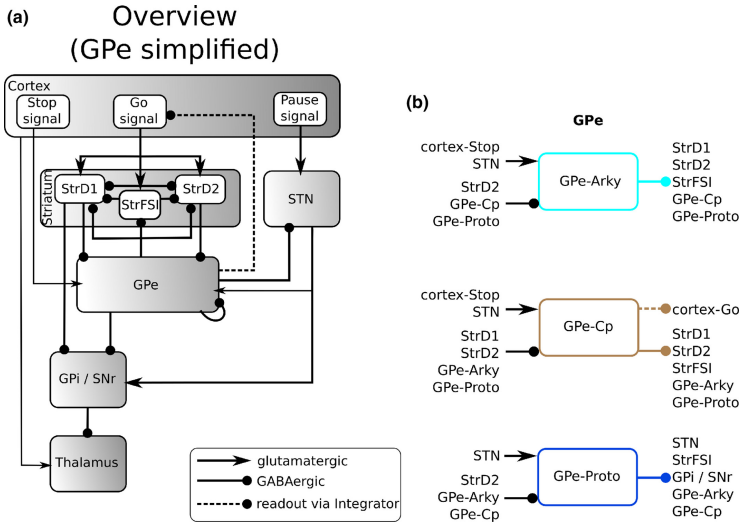

Figure 6: a) Interaction between different subpopulations on a generalized level, indicating the polarity and direction of the interaction. Synaptic weights and number of connections on a neuronal basis are not presented and can be found in the sections below. b) Inputs and outputs of the three different GPe subpopulations indicating the origin of the afferent projections and the target of the efferent projections. GPe intraconnectivity is accomplished via connections between the subpopulations. Originally published in Goenner et al. [8]

$$\frac{du}{dt} = a(bv - u) \tag{2}$$

$$\frac{dg_{AMPA}}{dt} = \frac{-g_{AMPA}}{\tau_{AMPA}} + H^{syn}_{AMPA} + I^{ext} \tag{3}$$

$$\frac{dg_{GABA}}{dt} = \frac{-g_{GABA}}{\tau_{GABA}} + H^{syn}_{GABA} \tag{4}$$

These formulae hold for all neurons in the model with the exception of the striatal neurons, which use the following expression for the recovery variable u:

$$\frac{dU}{dt} = a(b(v - (-80)) - u) \tag{5}$$

In the Izhikevic equations v and u are dimensionless variables and n_2, n_1 and n_0 are dimensionless parameters fitted to specific cell types which govern the membrane dynamics and scale the system of equations to biophysical voltage ranges for v in mV and to ms for t [15]. In this system of equations the introduction of additional terms requires units to be ascribed to these parameters. This leads to the following units for the variables and parameters; $v(mV)$, $u(mV)$, $n_2(\frac{S}{m*V})$, $n_1(\frac{S}{m})$ and $n_0(A)$. g_{AMPA} and g_{GABA} are the conductivity variables in $\frac{S}{m}$ for the AMPA and GABA gates with $E_{AMPA} = 0mV$ and $E_{GABA} = -90mV$ being their respective Nernst potentials. Finally C is the capacitance of the membrane

Table 1: Parameters for Izhikevic Spiking Neurons, on a population basis. Parameter set as used in Goenner et al. [8].

Population	a(-)	b(-)	c(-)	d(-)	n_0(A)	$n_1(\frac{S}{m})$	$n_2(\frac{S}{m*V})$	C (F)	V_{peak} (mV)
STR(D1/D2)	0.05	-20	-55	377	61.651	2.595	0.0228	50	40
FSI	0.2	0.025	-60	0	43.75	1.5	0.0125	25	80
STN	0.005	0.265	-65	2	140	5	0.04	1	30
GPi	0.005	0.585	-65	4	140	5	0.04	1	30
GPe-Proto	0.0058	0.56	-65	3.8	117	4.86	0.043	1	30
GPe-Arky	0.0054	0.34	-71	9.81	113	4.47	0.04	1	30
GPe-CP	0.0058	0.56	-65	3.8	117	4.86	0.043	1	30
Thalamus	0.02	0.2	-65	6	140	5	0.04	1	30

in F. The recovery variable change is influenced by specific recovery parameters a and b which are dimensionless parameters. The decay rate of the conductivity variables are given by their time constants $\tau_{AMPA} = 10ms$ and $\tau_{GABA} = 20ms$. The Nernst potentials and time constants for the AMPA and GABA channels are equal across all cell types. The values for the celltype specific parameters are given in Table 1

If $v > V_{peak}$, then $v = c$ and $U = U + d$. In this event the neuron is considered to have spiked for the purposes of neuron interaction. The values for c and d are dimensionless population dependent parameters which determine the state of the membrane potential and recovery variable after this event has occurred. Neuron interaction is facilitated through the gating channels, with AMPA facilitating excitation of the target neuron and GABA facilitating inhibition of the target neuron. The general formula for the change in AMPA or GABA conductivity is as follows:

$$H^{syn} = s * w_{i \to j} * \sigma \tag{6}$$

Here $s = 2.5$ is the dimensionless scaling factor to account for the differences in timescale between the current model and the parameters as given in Goenner et al., $w_{i \to j}$ is the dimensionless weight factor for synaptic interaction from spiking neuron i to target neuron j, and σ is the sigmoid transmission variable ranging from 0 to 1. H is a function of the membrane voltage of the projecting neuron at some delay $\tau d(ms)$ in the past. It is given in the following expression:

$$\sigma = \frac{1}{1 + e^{\beta * (v(t - \tau d) - (v_{peak} - 10))}} \tag{7}$$

The peak voltage $V_{peak}(mV)$ is the value at which the membrane voltage is reset and is considered the threshold for action potential. The time delay τd in ms is chosen from a uniform random distribution in the range of 1 to 10 for every neuron. The sloping factor β gives the steepness of the sigmoid function and is set to -10.

In the paper by Goenner et al. [8] baseline activity is achieved through the application of external currents to the neurons based on their type. This was done by having neurons with consistent spiking frequency project to single neurons. The frequency was population specific and pulled from a Poisson distribution ensuring diversity of baseline activity. Modelling additional neurons solely for the purpose of providing input to single neurons inserts complexity and would increase the simulation workload. To simplify establishing baseline activity, predetermined spike trains will be applied to the neurons during the simulation. The frequency of these spike trains is based on the spike frequency of the input neurons. The pulse width is determined to be 0.1 ms, which is the size of a single time step in the Goenner et al. model. The value of the gating variables is only increased at the instant of action potential transmission. The amplitude of the pulses is determined by the synaptic weight of the input neurons. Similarly, input into the system will be applied via the use of precalculated pulsetrains to the AMPA gates of the target neurons.

2.3 Neural Connectivity

In this section the connections between the subpopulations of the BG will be explained in terms of afferent projections. Every population receives AMPA input meant to simulate a superposition of the ever-present cortical activity and induce a baseline activity. Details on this baseline inducing input will be discussed below, in the Simulation Protocol. The synaptic transmission weights and integrator input values are given in Table 2.

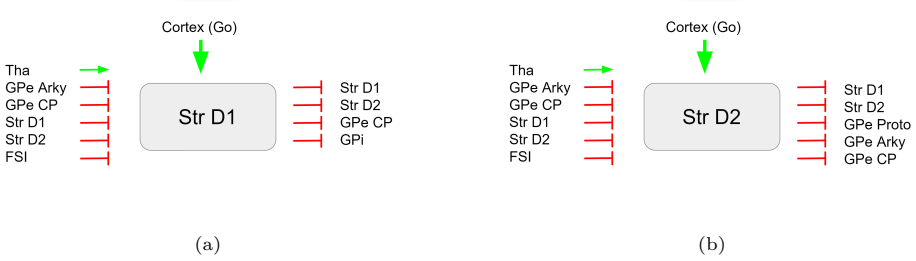

Figure 7: A connectivity scheme for the striatal MSN populations. While the inputs into both a) the D1-Type MSNs and b) the D2-Type MSNs are the same, they have differences in target populations. The green arrow indicates an excitatory projection and the red line indicates an inhibitory projection. Input coming from above indicates external stimulation from the cortex as well as which specific signal this corresponds to.

2.3.1 Striatum

The striatum consists of two populations of medium spiny neurons (MSNs), D1-type DA-receptor expressing MSNs and D2-type DA-receptor expressing MSNs, henceforth referred to as StrD1 and StrD2 respectively. The StrD1 and StrD2 populations each receive inhibitory projections from two neurons within their own subpopulation and two neurons between subpopulations. Additionally, they

receive three inhibitory neuron projections each from the GPe-Arky and three inhibitory projections each from the GPe-CP subpopulations. Lastly, they each receive two inhibitory projections from the FSIs. The thalamus sends two excitatory projections to each of the striatal subpopulations. The striatum is historically the major input site of the BG, and as such the glutamatergic Go signal will be applied to the striatal MSNs of both populations. The striatum is the only nucleus of the BG in this model does not have its connections restricted to a single pathway. The interpopulation and intrapopulation inhibitions of the striatum are across the entire node. The projections originating from downstream nuclei are restricted exclusively to their own pathway and will only affect the striatal neurons within their own pathway. Thus, the striatum is the hub within the BG where the parallel pathways can interact with each other, albeit within the restrictions mentioned here. The connectivity scheme for both MSN populations can be seen in Figure 7.

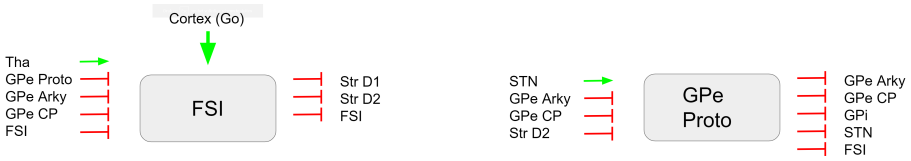

(a) (b)

Figure 8: A connectivity scheme for the striatal FSI population and the prototypical GPe subpopulation. The green arrow indicates an excitatory projection and the red line indicates an inhibitory projection. Input coming from above indicates external stimulation from the cortex as well as which specific signal this corresponds to.

2.3.2 Fast Spiking Interneurons

The Fast Spiking Interneurons are a small portion of the overall population of the striatum. They receive two inhibitory projections from other FSIs. The three GPe populations send three inhibitory projections each to a FSI. Additionally, they receive the same cortical stimulation as the other striatal populations as well as two excitatory projections from the thalamus. In contrast to the MSNs, the FSIs do not send interpathway projections and only inhibit within their own pathway. A connectivity scheme for this population can be seen in 8a.

2.3.3 GPe-Proto

The prototypical GPe neurons receive inhibitory inputs from the two other GPe subpopulations, three projections from each. Additionally it receives two inhibitory projections from the StrD2 neurons. The GPe-Proto neurons receive three excitatory projections from the STN. A connectivity scheme for this population can be seen in 8b.

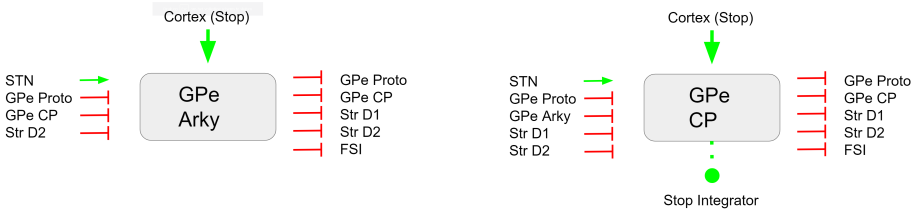

Figure 9: A connectivity scheme for the arkypallidal GPe subpopulation and the cortico-pallidal GPe subpopulation. The green arrow indicates an excitatory projection and the red line indicates an inhibitory projection. Input coming from above indicates external stimulation from the cortex as well as which specific signal this corresponds to. The dotted line to the bottom indicates this node sends input to the Stop integrator.

2.3.4 GPe-Arky

The arkypallidal GPe neurons receive inhibitory inputs from the two other GPe subpopulations, three projections from each. It receives two inhibitory projections from the StrD2 neurons. The GPe-Arky neurons receive three excitatory projections from the STN and are one of the two input sites for the glutamatergic Stop signal from the cortex. A connectivity scheme for this population can be seen in 9a.

2.3.5 GPe-CP

The cortico-pallidal loop GPe neurons receive inhibitory inputs from the other two GPe subpopulations, three projections from each. Additionally it receives two inhibitory projections from the StrD2 neurons and two inhibitory projections from the StrD1 neurons. The GPe-CP neurons receive three excitatory projections from the STN and are the other input site for the glutamatergic Stop signal originating in the cortex. A connectivity scheme for this population can be seen in 9b.

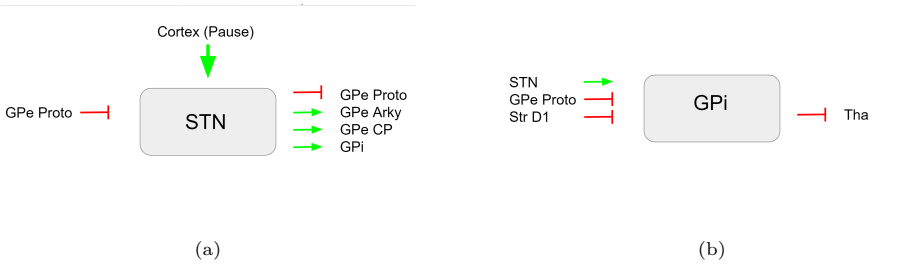

Figure 10: A connectivity scheme for the STN population and the GPipopulation. The green arrow indicates an excitatory projection and the red line indicates an inhibitory projection. Input coming from above indicates external stimulation from the cortex as well as which specific signal this corresponds to.

2.3.6 STN

The neurons in the subthalamic nucleus receive three inhibitory projections from the GPe-Proto neurons. The STN is the other major input site of the BG, with the hyperdirect pathway finding its origin here. As such, it is the sole input site for the diffuse, cortical excitation which is applied before the arrival of the Go or Stop Signals. A connectivity scheme for this population can be seen in 10a.

2.3.7 GPi

The GPi receives two inhibitory projections from the StrD1 neurons as well as three inhibitory projections from the GPe-Proto neurons. It receives excitatory projections from three STN neurons. A connectivity scheme for this population can be seen in 10b.

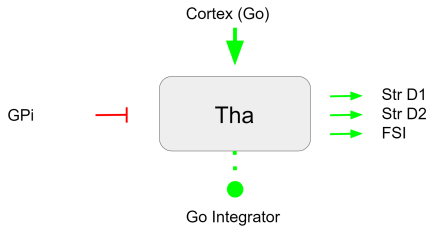

Figure 11: A connectivity scheme for the thalamic population. The green arrow indicates an excitatory projection and the red line indicates an inhibitory projection. Input coming from above indicates external stimulation from the cortex as well as which specific signal this corresponds to. The dotted line to the bottom indicates this node sends input to the Go integrator.

2.3.8 Thalamus

The Thalamus receives three inhibitory projections from the GPi neurons. It receives excitatory input from the Go signal at the same time as the striatal neurons. A connectivity scheme for this population can be seen in 11.

2.3.9 Model Outputs

There are two primary output nodes in this model, which are modelled as integrators. These nodes each receive input from a single population within the model. The first is the Go integrator, which receives input for every single spike produced by the thalamus. The second is the Stop integrator, which receives input for every spike produced by the GPe-CP population. The Stop integrator has an additional interaction with the model. If one of the Stop integrators for any given path reaches a certain threshold value it will stop the Go signal from having effect by applying the falling phase of the Go signal from that point in time onward. It should be noted that a set integrator exists for each and every

pathway. The Go integrator is only indicative of a Go signal passing through a single pathway. The Stop integrators have a global effect. For instance, if the Stop integrator for path 3 were to reach the designated stop threshold, this event will trigger the cessation of the Go signal for all pathways.

Table 2: Connectivity strengths between pre- and postsynaptic neurons based on the BG subpopulation. These values are used in eqn. 6 in the function for gate conductivity. Originally published in Goenner et al. [8].

Presynapse	Postsynapse	$w_{Pre \to Post}$	Receptor
StrD1	GPi	0.06	GABA
	StrD1	0.01	GABA
	StrD2	0.015	GABA
	GPe-CP	0.005	GABA
StrD2	StrD1	0.015	GABA
	StrD2	0.01	GABA
	GPe-Proto	0.04	GABA
	GPe-Arky	0.08	GABA
	GPe-CP	0.08	GABA
FSI	StrD1	0.01	GABA
	StrD2	0.01	GABA
	FSI	0.01	GABA
STN	GPi	0.04	AMPA
	GPe-Proto	0.001	AMPA
	GPe-Arky	0.001	AMPA
	GPe-CP	0.001	AMPA
GPe-Proto	STN	0.001	GABA
	GPi	0.015	GABA
	FSI	0.02	GABA
	GPe-Arky	0.025	GABA
	GPe-CP	0.025	GABA
GPe-Arky	StrD1	0.065	GABA
	StrD2	0.12	GABA
	FSI	0.08	GABA
	GPe-Proto	0.008	GABA
	GPe-CP	0.008	GABA
GPe-CP	StrD1	0.01	GABA
	StrD2	0.01	GABA
	FSI	0.01	GABA
	GPe-Proto	0.008	GABA
	GPe-Arky	0.008	GABA
GPi	Tha	0.06	GABA
Tha	StrD1	0.14	AMPA
	StrD2	0.12	AMPA
	FSI	0.12	AMPA

2.4 Model Parameters

The model presumes the neuronal populations to have different parameters on a population level. The parameters are based on the model of Goenner et al. [8]. Whenever there is a deviation from this model it will be mentioned in text.

The parameters for the Spiking Izhikevic Neurons all populations are given in Table 1. The main alteration in the model compared to Goenner is the reduced complexity of the population scheme. For this reason, the GPe parameters are based on the parameters given for prototypical GPe neurons.

2.5 Stop Signal Reaction Time

To calculate the Stop Signal Reaction Time (SSRT) two relationships must be established. Firstly the distribution of Go reaction times (GORT) must be determined. This will be done by collecting the GORTs from Go Trials and determining the probability distribution. Secondly the relationship between the probability of inhibiting the Go response and the Stop Delay (SD) must be established. In the ideal scenario the SD for which the probability of inhibition is 50 % will be determined. In which case the SSRT can be calculated as follows:

$$SSRT = \mu_{GORT} - SD \tag{8}$$

The SSRT, μ_{GORT} and SD are all given in ms.

2.6 Local Field Potential Approximation

A Local Field Potential (LFP) is a common measure of neuronal activity extracted from small brain regions using small electrodes. It is the total sum of the electrical field potentials generated by the neurons in a small volume of space surrounding the sensor. It is possible to calculate an approximation of the LFP using data obtained from the simulations, which is useful in identifying signal characteristics of a population or group of neurons, as opposed to the single cell recording approximations otherwise available. Parasuram et al. [28] detailed a method used in the development for the tool LFPSim. Simplifying the formulae to disregard the spatial orientations of the neurons will still allow an approximate to be calculated, albeit one that considers all neurons to be equidistant to the sensor. Taking the following formulae:

$$I_{transmembrane} = I_{ionic} + c_m \frac{\partial V_m}{\partial t} \tag{9}$$

$$\Phi_{LFP} = \sum_{i=1}^{nsources} \frac{I_i}{4\pi\sigma r_i} \tag{10}$$

Here Φ is the extracellular potential measured at distance r for any given cell. The transmembrane and the ionic currents are used to calculate the voltage differential within the differential equation solver. This voltage data needs to

be resampled due to the nonuniformity of the timesteps. This can then easily be summed to obtain Φ. Assigning any particular value of r to the neurons would be arbitrary, thus it is fair to assume all neurons to be at the same distance to the sensor, or far away enough that the differences are negligible. It can similarly be assumed that the conductivity of the medium, σ, for the simulation environment is 1. Leaving the following equation for the approximation of a LFP for the simulated neurons:

$$\Phi_{LFP} = \sum_{i=1}^{n=populationsize} \frac{c_m \frac{dV}{dt}}{4\pi} \tag{11}$$

Once the LFP for a single population has been calculated it is possible to perform a frequency analysis. This LFP will then be filtered using Butterworth filters. The second-order high pass filter has a cut-off frequency of 10 Hz and the sixth-order low pass filter had a cut-off frequency of 600 Hz, the transfer function for both filters were calculated for a sampling frequency of 10 kHz. Finally, after filtering, the frequency analysis can be performed using the Continuous Wavelet Transform.

2.7 Model Simulations

Using the model described above, a series of Stop Signal Tests are performed for two conditions. A control case, using the architecture as described earlier, and a parkinsonian case, including dopamine dependent connectivity scaling within the striatum, details of which will be described below. For both of these conditions Go Trials will be used to determine the mean and variance of the GORT. The Stop Trials will yield a successful stop or a failed stop yielding a GoRT. A desirable error rate is approximately 50%, during simulation this can be approached by shortening the SD after failed stop attempts and lengthening the delay after a successful stop by a fixed value of 10 ms.

2.7.1 Normal Condition

To simulate the competition between parallel functions within the BG the cortical input acting as the Go signal is given to each pathway simultaneously. The predetermined 'irrelevant' responses are given a salience thrice as low as its 'correct' competitor. These signals simulate competing non-relevant actions and effectively act as noise. The Stop signal is given equally to all pathways in response to the Stop integrator reaching threshold value for any pathway. The cortical input is modelled as a superposition of synaptic inputs from cortical populations onto the AMPA receptors of the target populations. This signal has two distinct phases; a rising phase and a falling phase, the length and slope of which depend on whether it simulates a Pause signal, a Go signal or a Stop signal. The function for the spiking frequency of the input signal is as follows:

$$\frac{\partial y}{\partial t} = \frac{r_{target} - y}{\tau} \tag{12}$$

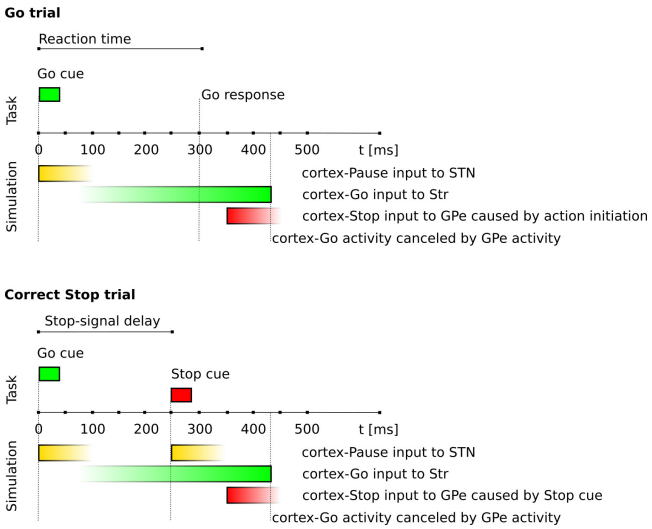

Figure 12: The order and salience of the various inputs for both trial scenarios are presented, with t = 0 defined as the Go cue. The opacity of the colours represents the relative input strength at that point in time. The delays between the inputs is fixed, other than the Stop Signal Delay, which is dynamically altered in between Stop Trials. This sequence of events was originally used in Goenner et al. [8]. The signal train in this experiment follows the depicted relations and events, with the exception of the GPe-CP feedback halting striatal input in Go Trials.

In this equation r_{target} is the target spiking rate and τ is the time constant. The values for the input signals can be found in Table 3. It should be noted that while the Pause and Stop signals are transient, the Go signal will enter its falling phase only when the Stop event triggers. This means that the Go signal will continue to trend towards its target frequency for the duration of the trial unless it is interrupted and shifted into its falling phase due to a Stop integrator reaching its threshold value.

A visual representation of the general signal flow can be seen in Figure 12. In absence of an external Go cue, the trial starts at a fixed point after the simulation has started. A delay of 100 ms has been chosen to allow the variables to reach an equilibrium and prevent any start up artefacts. At this moment cortical input into the STN marks the start of the trial, referred to as the Go cue. This STN input is short lived and is succeeded by an input of ever increasing salience into the striatum. The striatal input is given after a short delay of 75 ms. This delay is in place to mimic the timing difference between the inputs to the hyperdirect pathway and the striatum. In Go Trials, the striatal input will continue on uninterupted and after a certain period an action will be detected on the thalamus via the Go integrator when this reaches a value of 0.13. In contrast to the original simulations performed in Goenner et al. there is no feedback event from the GPe nodes in Go trials. As such the striatal input will continue on unabated for the remainder of the simulation. The differs from the

signal scheme presented in Figure 12, but seeing as the total trial time for these simulations is shorter, at 600 ms in total, this should not affect the outcome, as the trial will end shortly after a Go response either way.

Stop trials begin in the same way as Go trials, with cortical input into the STN followed by striatal stimulation after a short delay. The Stop cue is defined as the moment a second burst of input is presented to the STN. The delay between the Stop and Go cues is defined as the Stop Delay. The Stop delay is altered dynamically between trials depending on the success or failure of inhibition in the preceding trial in the series, the value is initialized as 150 ms. The SD is increased by 10 ms if the preceding trial was successful and decreased by 10 ms if the preceding trial failed to inhibit. Cortical input to the GPe-Proto and GPe-CP is presented after a fixed delay of 50 ms. This delay is designed to mimic the timing differences between the fast hyperdirect input and the relatively slower cortical inputs to the other parts of the BG. Once the Stop integrator monitoring the GPe-CP node reaches a threshold value of 1.3 the GPe input is halted and the striatal input aborted, triggering the falling phase of the rate equations.

Table 3: These parameters determine the target spiking rate of the signal as well as the speed at which this target can be reached. Parameter values originally published in Goenner et al. [8].

Signal	Phase	$r_{target}(spikes/s)$	$\tau(s^{-1})$
Pause	Rising	500	1
	Falling	0	150
Go	Rising	400	200
	Falling	0	10
Stop	Rising	400	1
	Falling	0	70

2.7.2 PD Condition

The hallmark of PD pathology is the depletion of DA levels throughout the BG. This has a large impact on the neuronal dynamics of the system, especially within the striatum, where a large population of DA receptor expressing neurons reside. In D1-type expressing MSNs, the presence of DA increases the surface expression of AMPA receptors, increasing their general excitability. In D2-type expressing MSNs, the presence of DA reduce the surface expression of AMPA receptors, decreasing their general excitability. In a depleted situation this would impact the responsiveness to the cortical glutamate signals received by the striatum. This can be expressed by the following scaling factors:

$$f_{D1} = 1 - d \tag{13}$$

$$f_{D2} = 1 + d \tag{14}$$

where d is a scaling factor depicting dopamine level compared to the norm. This scaling factor is applied directly to the connectivity strength from the

cortex to the relevant striatal populations. In the control situation $d = 0$. In the PD condition, the ambient dopamine level is significantly lower compared to normal levels. This is especially true for the stage in PD where significant motor problems become apparent. For this reason, during simulations in the PD condition d was chosen to be 0.75. The scaling factor is the sole difference between the control and PD condition in this model.

2.8 Simulation Protocol

The amount of trials to simulate has been estimated based on results from a study performing GO/Stop trial by Van den Wilderberg et al. [37]. Using the SSRT for both the control and the PD conditions an estimated sample size of 13 using a standard, normally distributed, two-sided distribution. Given the assumption that about half of the Stop trials will yield a SSRT, this should be increased to 26 per condition. This will result in a total 104 simulations, 26 Go-trials and 26 Stop-trials, for both the control and Parkinsonian condition.

Before each simulation the initial parameters were randomized. Every neuron receives simulated cortical input to the AMPA-receptor to induce baseline activity. The frequency of this baseline activity was a constant value chosen from a normal distribution described by the value given in Table 4. The neuron connectivity matrix was randomized as well. For every subpopulation the list of afferent projections was randomly generated, after which it was adjusted to ensure no neuron receives input from multiple instances of a single neuron. The number of projections is described above. Lastly, the initial values of the membrane potential V and the recovery variable U were randomly generated. The membrane potential was pulled from a uniform distribution with a range of -65 to -25 mV. The recovery variable was generated from a uniform distribution with a range of 60 to 100, with the STN being a exception, having the recovery variables for this nucleus pulled from a range of 35 to 45. The starting values for the recovery variables were determined from testing the resting state values of the model. Starting the variable around this range accommodates faster initialization in the presignal stage of the simulation. At the end of every simulation the results from the delayed differential equation solver as well as the current stop delay, in case of a Stop trial, were saved before another trial was initiated.

2.9 Statistical Analysis

The distribution of the test results was tested for normalcy using the Shapiro-Wilk test. Depending on the outcome, different methods will be used to determine significance of between groups. For normally distributed outcome parameters the two sample Student's t-test will be used to test for statistical differences between the two conditions. For non-normally distributed data, significance testing will be performed using the two-sided Wilcoxon rank sum test. All results will be tested for a significance level of $\alpha = 0.05$.

Table 4: Parameters for the spike firing rate and input strength of the cortically induced baseline activity. Originally published in Goenner et al. [8].

Population	w_{Input}	μ	σ
STR D1	0.7	10	2
STR D2	0.8	10	2
FSI	0.8	10	2
STN	0.2	400	80
GPi	1	400	80
GPe-Proto	100	400	80
GPe-Arky	90	400	80
GPe-CP	100	400	80
Thalamus	0.35	150	30

3 Results

3.1 Stop Signal Test Performance

Over the course of the experiment a total of 60 simulations were run and the test outcomes were generated as described in the method section previously. Ten Go signal-simulations were generated for both the control and parkinsonian conditions. Twenty Stop-signal simulations were generated for both the control and parkinsonian conditions. The amount of successful stop trials differed between the two conditions, ten out of twenty successful Stop Trials for the control condition, and twelve out of twenty successful Stop Trials for the parkinsonian condition. The decision was made to forego generation of additional Stop Trials due to time constraints.

The GoRTs were based on whether the Go-integrator exceeded the threshold value of 0.13 and the first instance this occurred during the simulation. Figure 13 shows the integrator values over time, for both conditions. The definition of a successful stop is based on the absence of a registered GoRT. Overall, the thalamic activity for both conditions as measured via the Go Integrator values are highly similar on first inspection as can be seen in Figure 14.

The Stop integrator values indicating the activity of the GPe-CP population at a given time are shown in Figure 15. It is plainly visible that this population is most active during Stop Trials. The moment the threshold value of 1.3 is exceeded seems to differ between successful and unsuccessful Stop Trials, though this is obfuscated by dynamically changing SDs, and as such no meaningful difference could be discerned from simple visual inspection. There is an interesting difference between the Stop integrator values during Go Trials between the control and PD conditions. In Figure 16 it can be seen that GPe-CP activity seems to remain stable over the course of the trial for the control condition. This contrasts with the integrator values diminishing as time goes on in the PD condition.

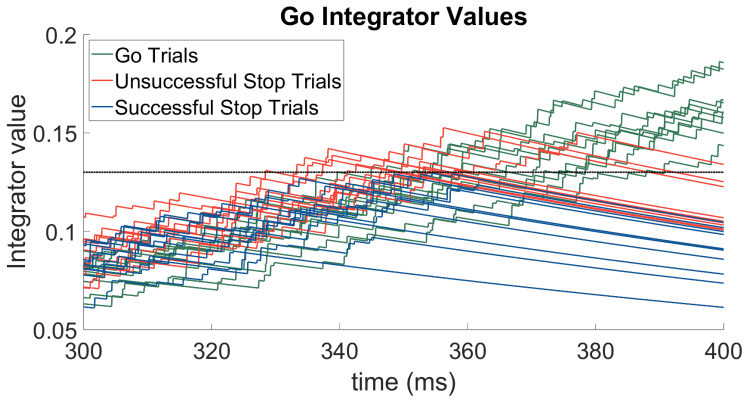

(a) Control

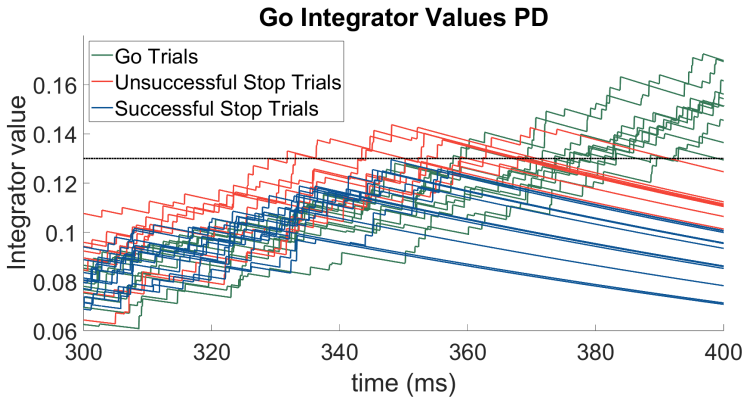

(b) Parkinson's Disease

Figure 13: Go Integrator values for both the a) control and b) parkinsonian conditions. These values are a measure of thalamic activity at a given point in time and are used to determine whether or not an action has occurred. If the integrator value crosses the threshold value of 0.13 at any point during a simulation, an action is said to have occurred at that point in time.

The Go Reaction Times, the Stop Error Reaction Times and the Stop Delay values were all tested for normality. The outcome of these tests can be found in Table 5. Due to failure to reject the null hypothesis, further analysis of this data will be performed using the two-sample Student's t-test.

Table 5: Test results of the Shapiro-Wilk test of normality of the distribution. Rejection of the null-hypothesis indicates a non-normal distribution. None of the experimental outcomes can be rejected as normally distributed.

	Control (p-value)	PD (p-value)
GORT	0.81	0.40
Stop Error RT	0.11	0.66
Stop Delay	0.12	0.10

Table 6: GORT: Go Reaction Time; primary response time during a Go trial. SD: Stop Delay; delay between to occurrence of a Go signal and a subsequent Stop signal. Stop success; amount of times a response has been successfully inhibited during a Stop Trial. Stop Error RT; the reaction time of the primary response in spite of a presented stop signal. SSRT: Stop Signal Reaction Times; calculated time it takes for a stop signal to result in a successful inhibition. * A t-test was not performed for statistical analysis of the SSRT values, however the 95 % confidence intervals were calculated giving the following results for the control, 101.8 $+/-$ 13.9, and PD, $112.7 + / - 10.5$, conditions it can be found that due to the overlap in ranges there is decisively no statistical significance.

	Control $\mu(\sigma)$	PD	p
GORT (ms)	262.8 (10.1)	274.8 (10.1)	0.0431
SD (ms)	161.0 (11.6)	162.1 (9.7)	0.7699
Stop Success (n)	10	12	-
Stop Error RT (ms)	244.5 (9.4)	250.0 (13.8)	0.3284
SSRT (ms)	101.8 (18.4)	112.7 (14.0)	*

3.1.1 GORT vs. Stop Error RT

One of the assumptions of the Stop Signal ask is the presence of a consistent GoRT probability distribution between the Go and the Stop trials. One way to check for this is to compare the reaction times between the Go trials and the Stop Error reaction times. According to the theory, the Stop Error reaction times come from the lowest 50% of the primary reaction time distribution and should therefore have a statistically significant difference. In Figure 17 it can be seen that there is a noticeable difference between the primary reaction time and the Stop Error reaction time. Statistical analysis yields a p-value of 0.0033 for the control condition and $4.4e^{-4}$ for the parkinsonian condition. These results indicate that the Stop Signal tasks have been successfully simulated.

3.1.2 Parallel Pathway Activation

The model simulated the Stop Signal task with the existence of parallel pathways corresponding to non-relevant, competing functions. The Go signal for the 'correct' pathway was significantly higher compared to the competing parallel paths. In this simple experimental design, there were no occurrence of a 'wrong' action being chosen. The Stop signal and Pause signals, by contrast, were applied equally to all channels in accordance with the Centre Surround model

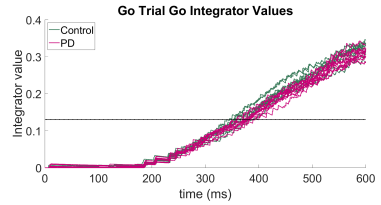

(a) Go Trial

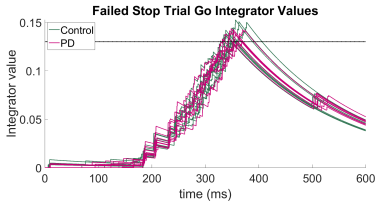

(b) Failed Stop Trial

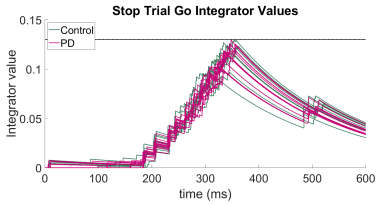

(c) Stop Trial

Figure 14: Go Integrator values over time for a) Go Trials, b) Failed Stop Trials and c) Successful Stop Trials for both the control and parkinsonian condition.

of action selection within the BG. A comparison between the Go integrator values of the multiple pathways can be seen in Figure 18. Here it can be seen that although there is activity for undesirable actions, they would not reach the threshold to become activated within the time span of the simulation, even were the desired action absent.

The Stop integrator activities for the different pathways are more evenly matched. In the majority of instances, in both control and PD condition, the stop integrator on Path 1 initiated the cessation of the Go signal. This does not necessarily mean the action was successfully inhibited, merely that the stopping threshold was reached. There were five instances of the stopping threshold not being reached in the control condition. These five instances also correspond with a successful inhibition. The same is true for the PD condition where there were two instances of the stopping threshold not being reached, but the inhibition being successful nonetheless. In the control condition, there was one instance of the stop being initiated by a pathway other than Path 1 and two instances of multiple pathways reaching the threshold at approximately the same time. In the Parkinsonian condition, there was also one instance of a pathway other than Path 1 being solely responsible for the cessation of the Go-signal. The amount of times multiple pathways reached the threshold nearly simultaneously was higher, occurring six times.

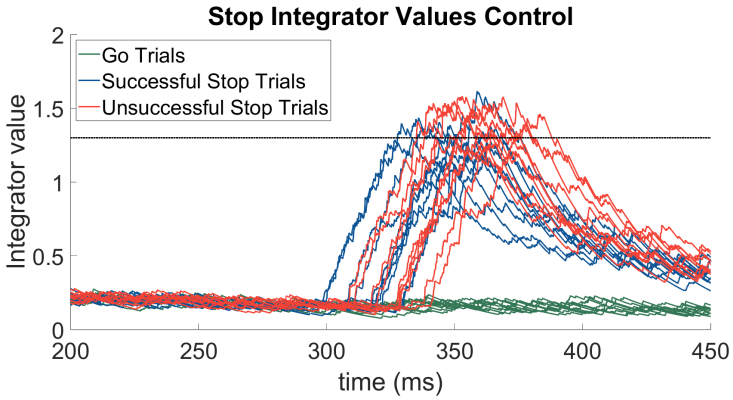

(a) Control

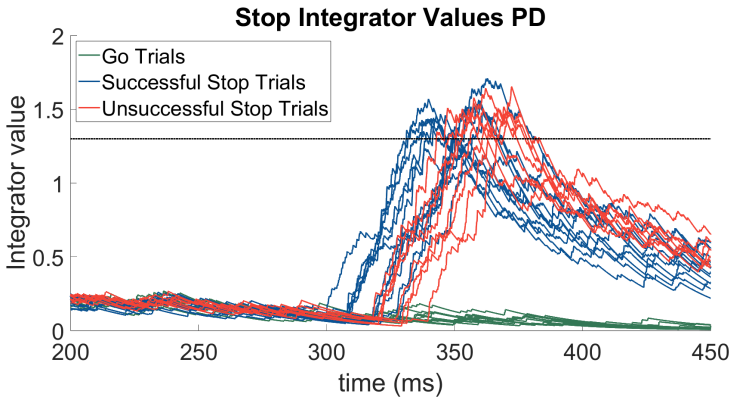

(b) Parkinson's Disease

Figure 15: Stop Integrator values for both the a) control and b) parkinsonian conditions. The if at any point during the trial the threshold value of 1.3 was crossed, the stopping procedure would be started and all input into the model would soon come to a halt.

3.2 Wavelet Analysis

To better understand the dynamics present within the model and the dynamics of the populations within the network a wavelet analysis was performed. The raw data obtained from the simulations were resampled at 10kHz at a three to one ratio. Firstly, the individual neuron data was translated to a Local Field Potential (LFP) approximation on a neuronal population basis. The signal was filtered successively with the Butterworth filters described above. Additionally, first 15 ms of the signal were omitted from the frequency analysis due to the presence of fairly significant step-in artefacts at the start of the simulation. A continuous wavelet transformation using the Morlet waveform was performed on the LFPs of single trials.

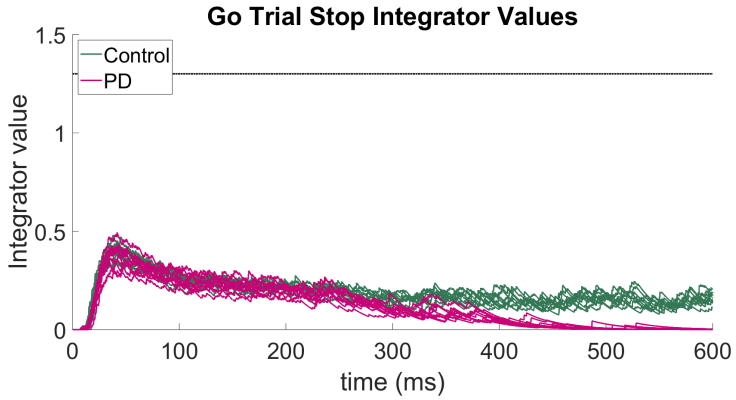

Figure 16: Stop Integrator values over time for Go trials for both the control and parkinsonian conditions. There is no period of elevated activity in the GPe-CP, as can be expected from the absence of a cortical Stop input. However, the control condition seems to maintain a steady level of activity in comparison to the PD condition, where activity diminishes over time.

3.2.1 Go versus Stop Trials

The moment the pause signal is applied to the STN is clearly distinguishable in both the Go and Stop trials through the short burst of high frequency around 400 Hz, see Figure. At the same time there is a noticeable increase in power in the lower frequencies as well. This process is the same for both the control and Parkinsonian condition.

The other major input site of the model is the striatum, with each of the three striatum subpopulations receiving nearly identical cortical input. There is only a slight difference in the synaptic weight of the input, in the control condition. The FSI population does not add much to the dynamics of the model, never reaching an active state and therefore not communicating with other neurons. It does however receive input identical to the D1 and D2 type MSNs, allowing for comparison between these populations and allowing the separation of effect from the input and the dynamics between neurons, to a certain degree. This is illustrated in Figure 20 where the higher frequency content is similar in all three populations, but there is a notable presence of lower frequency content in the MSNs as compared to the FSI populations.

Using the CWT the cortical inputs in to the system and the timings become more easily apparent. Visual analysis alone, however, does not suffice for comparison of frequency spectra between the control and parkinsonian conditions. To attempt this, comparisons of the power spectra between the Go Trials of both conditions has been performed. Two specific bands of frequencies were selected to compare between the two conditions, namely the frequencies corresponding to beta brainwaves (15 - 30 Hz) and the lower range of gamma brain waves (30 - 60 Hz). These bands have been selected for the following reason. These frequency ranges were unaffected by the filtering process and originated

Figure 17: Boxplot of the Go Reaction times and Stop Error reaction times both the control and Parkinsonian condition. *: mean population difference with $p < 0.05$. **: mean population difference with $p < 0.01$.

from the dynamics of the system. None of the cortical input frequencies to induce baseline activity were in this range nor do they appear in the FSI spectra. Furthermore, the beta band is frequently associated with PD, being implicated in various motor symptoms [26]. The Go Trials of both conditions are more easily comparable due to the lack of additional time varying aspects, as is the case in the Stop Trials with their variable SDs. The time window over which this analysis can be performed is bounded on both sides by the cone of influence produced by the CWT. The time window is narrowest at lower frequencies, as such, the boundaries for 15 Hz will be taken for all frequencies.

The average spectral power of the two conditions for both frequency bands can be seen in Figure 22 for the GPe subpopulations. The largest area of significant difference can be found in the striatal populations, with the D1-type MSNs having a larger window for beta frequencies and the D2-type MSNs having a larger area for the gamma frequencies, as can be seen in Figure 21. Notably, even though the location is most often associated with beta band frequencies in literature, the STN-GPe loop, there is hardly any difference between the band powers in the STN in either condition, especially when compared to the GPe-populations. It is interesting to note that while the GPi does display differences between the two conditions, the gamma band is the most affected, whereas the beta frequencies are largely comparable, as can be seen in Figure 23.

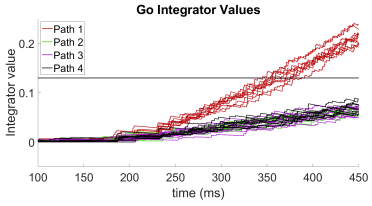

(a) Control Go Trial

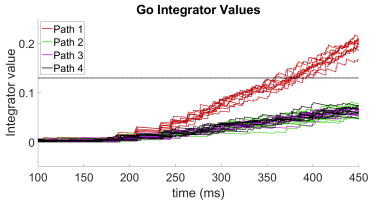

(b) PD Go Trial

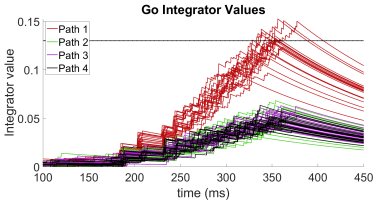

(c) Control Stop Trial

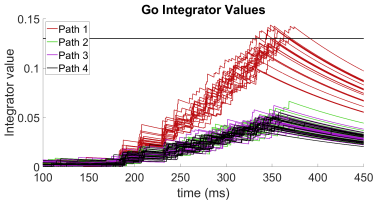

(d) PD Stop Trial

Figure 18: The value of the Go integrators over time for both conditions and both trials are depicted above. Path 1 represents the Go integrator values for the chosen correct pathway over time across the Go trial simulation for the healthy control. Path 2, 3, and 4 represent the additional competing actions. It can clearly be seen that in this experimental setup, the chance for selection of a irrelevant action is vanishingly small.

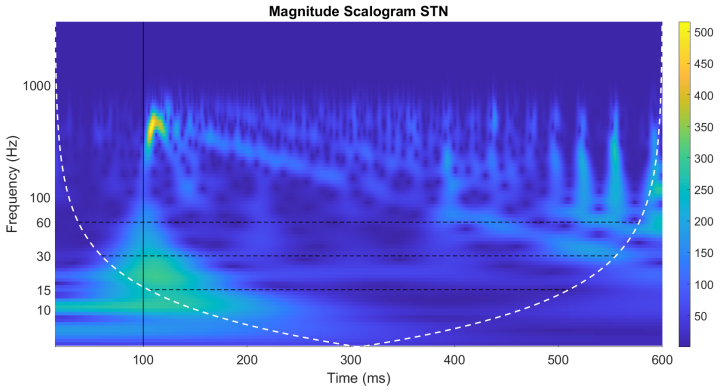

(a) Go Trial

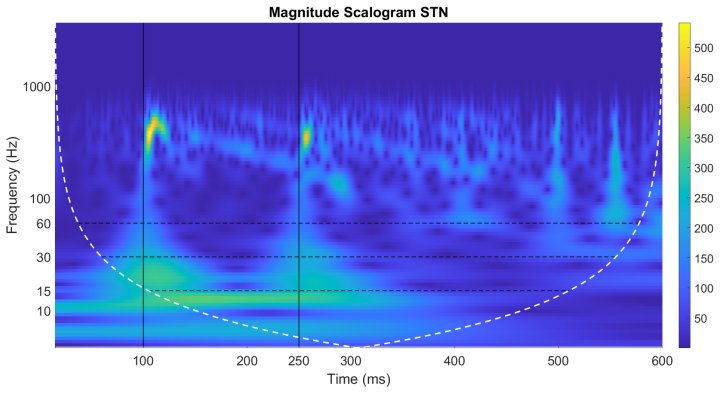

(b) Stop Trial

Figure 19: Continuous Wavelet Transformation Scalogram of the STN in the normal condition for both the Go and Stop trials. The vertical line at 100 ms indicates the initiation of the Go cue, which first gives a Pause signal to the STN. The Stop Trial (b) has a second vertical line at 250 ms indicating the initiation of the Stop cue, which gives a second Pause signal to the STN. The short burst of activity corresponding to the Pause signal is plainly distinguishable. The dashed lines indicate the frequency regions of interest, namely the beta band (15 - 30 Hz) and the gamma band (30 - 60 Hz). The white dashed shows the cone of influence, outside this line the CWT amplitudes are not significant.

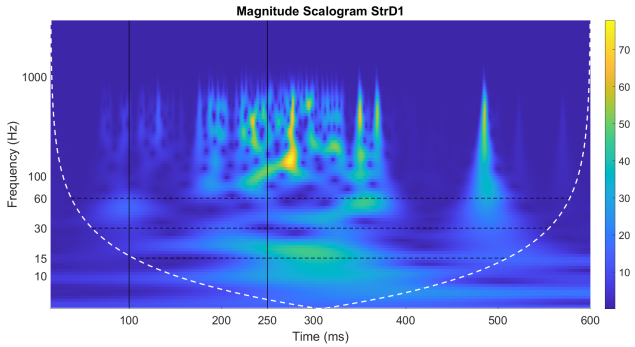

(a) D1 type MSN

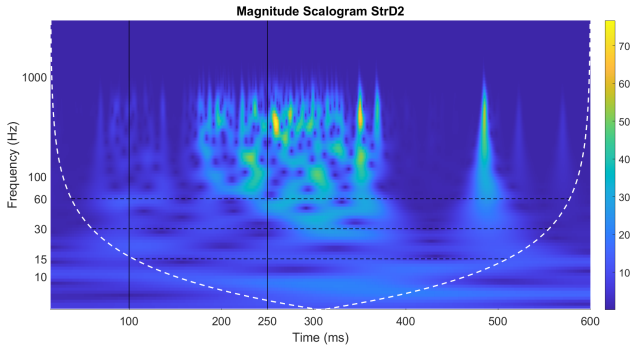

(b) D2 type MSN

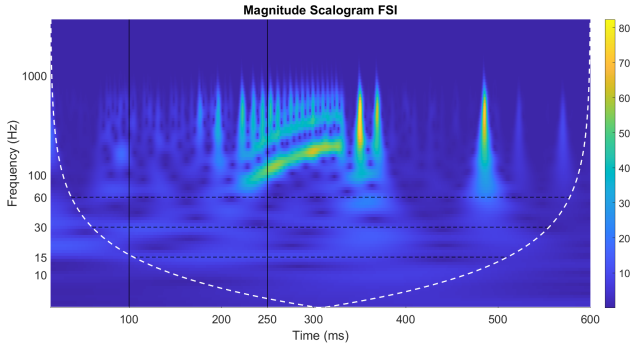

(c) Fast Spiking Interneurons.

Figure 20: Continuous Wavelet Transformation Scalogram of the Striatal populations in the normal condition for the Stop trials. The cortical input to the striatum is present in all three populations, but the lower frequency content is found mostly in the D1-type MSNs. The cone of influence is bounded by the white dashed border showing nonsignficant wavelets. The black vertical lines at t = 100 ms and t = 250 ms indicate the initiation of the Go cue and Stop cue respectively. The regions of interest the beta band (15 - 30 Hz) and the gamma band (30 - 60 Hz) are emphasized with the horizontal dashed lines.

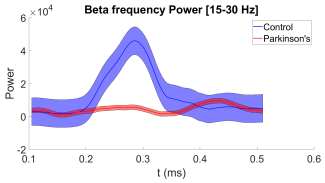

(a) Beta Band Power StrD1

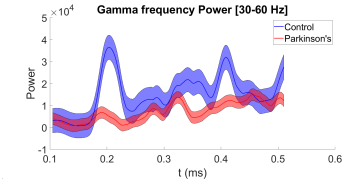

(b) Gamma Band Power StrD1

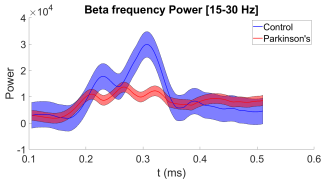

(c) Beta Band Power StrD2

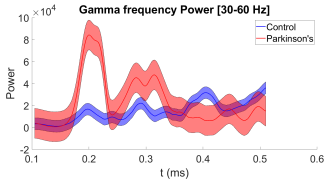

(d) Gamma Band Power StrD2

Figure 21: Average spectral power over time in the striatal subpopulations for both the Control and PD conditions. Shaded regions display the 95% CI. The left column displays beta band (15 - 30 Hz) power and the right column displays gamma band (30 - 60 Hz) power.

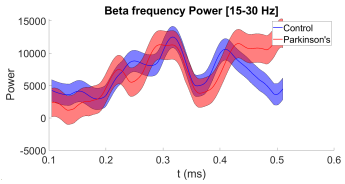

(a) Beta Band Power GPe-Proto

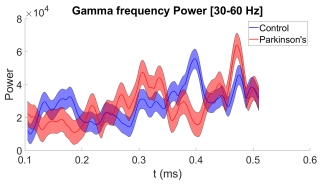

(b) Gamma Band Power GPe-Proto

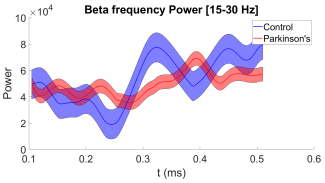

(c) Beta Band Power GPe-Arky

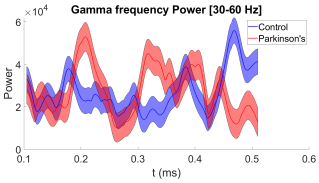

(d) Gamma Band Power GPe-Arky

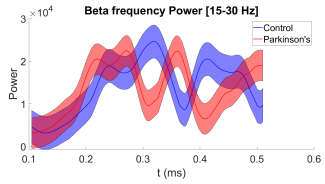

(e) Beta Band Power GPe-CP

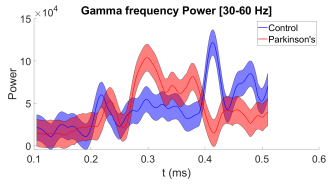

(f) Gamma Band Power GPe-CP

Figure 22: Average spectral power over time in the GPe subpopulations for both the Control and PD conditions. Shaded regions display the 95% CI. The left column displays beta band (15 - 30 Hz) power and the right column displays gamma band (30 - 60 Hz) power.

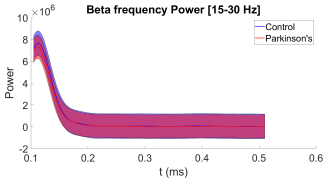

(a) Beta Band Power STN

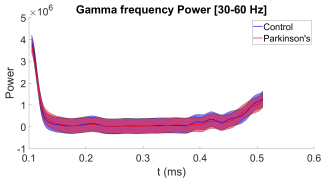

(b) Gamma Band Power STN

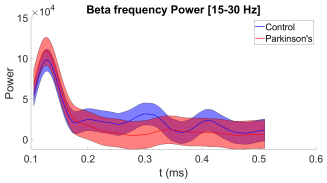

(c) Beta Band Power GPi

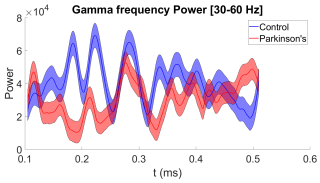

(d) Gamma Band Power GPi

Figure 23: Average spectral power over time in the STN and GPi populations for both the Control and PD conditions. Shaded regions display the 95% CI. The left column displays beta band (15 - 30 Hz) power and the right column displays gamma band (30 - 60 Hz) power.

4 Discussion

The aim of the research was to develop a model of the BG capable of simulating the Stop Signal task in both a control and parkinsonian condition. A few factors should be considered before definitively discussing the validity of the model. It should be noted that the model was able to faithfully reproduce the mathematical conditions of the Stop Signal task as outlined by Logan and Cowan. The GoRTs obtained from the trials followed a normal distribution and there was a significant difference between the primary reaction times for Go and Stop Trials. This held for both the control and the parkinsonian condition. A significant difference between the SSRTs could not be established, even though there was a significant difference between the GoRTs for the conditions. A major factor holding back further experimentation with this model is the computational expenses and the ability to generate enough data to establish statistical significance, if any should exist. Provided this obstacle could be overcome, this model could be used for different experiments regarding action selection in a time dynamic fashion.

The remainder of the discussion will detail some topics in depth, particularly expanding on the reasons for certain design decisions and assumptions, and the shortcomings of the current model as well as suggestions on how to overcome these. In the final section, suggestion for possible future steps in the utilization of the model will be given.

4.1 Validity of the results

It would be prudent to compare the results from this model with those of its inspiration. Goenner et al. did not incorporate any pathologies into their simulations, being primarily focused on the validation of their model in terms of the 'pause-then-cancel' model. They reported an average GoRT for Go Trials of 339.5 and an average GoRT for failed Stop Trials of 289.9. This constitutes a difference of 76.7 and 45.4 ms with the GoRT and Stop Error RT obtained from this model respectively.

Comparing the simulation results with experimental results obtained from real subjects there is once again a significant difference. Comparing the GoRTs with values obtained from a group of Parkinson's patients and age matched healthy controls, as performed by Gauggel et al. [7], real reaction times are nearly twice as high.

These differences seem to mostly depend on the time scaling of the simulations. The relationship between GoRT and Stop Error RT holds when compared to the model by Goenner et al. When adapting the model from the original equations some assumptions had been made in regards to the neural connections. The connectivity weights were maintained, but a gain factor had been added to make up for the differences in time scale and the possible effects this had on the equation solvers. This would affect the magnitude of the results, but should

have little impact on the difference in reaction times obtained from the same model.

There are also factors to consider when comparing simulation results with reality, namely that this model simulates the BG in isolation. In reality there are additional delays. The cues have to pass from the sensory organs to the brain, be recognized as relevant cues and then passed along the subcortical nuclei. After having passed through the relevant brain regions, the signals will have to travel to the muscles were a reaction may or may not be evoked. These processes, among others, introduce offsets to the reaction time when compared to models of brain regions in isolation. Attempts have been made to include some of these delays into the simulation of the Stop Signal task, specifically the delays between inputs arriving at the STN versus inputs arriving at the striatum.

If the ratio between the reaction times of PD patients versus healthy controls are compared to the model results, both cases have significant differences in reaction times with PD patients have slower GoRTs in general. It should be possible to approach similar model dynamics as in Goenner et al. if additional parameter fitting were to be performed with a specific focus on the time constants and connection gains.

Apart from this, little can conclusively be said about the validity of the experimental outcomes. The conditions regarding the mathematics have been met and given enough data it would likely be possible to perform Stop Signal task for various conditions. The internal workings of the model and the implementation of the Parkinson condition also require validation. Direct comparison of the LFP approximations and in-vivo measurements of the BG during Stop Signal tasks would be the most direct method. This data will most likely only be available for Parkinson's patients and not healthy controls due to the circumstances under which it can be collected. Furthermore, the main target of the majority of these studies is the STN, which in this model does not show a lot of difference between conditions. A number of recent studies has linked inhibition of actions during a Stop Signal task in PD patients with the dynamic presence of beta band power moments prior to inhibition [1] [29] [27] [41]. Currently it can be stated that the Pause signals in particular elicit significant bursts of beta and gamma band power for a short duration. Given more testing of the model it would likely be possible to compare the correlation of STN neurons during this period as well as how the level of beta band power correlates to successful inhibition. At the moment not enough testing has been performed to comfortably compare such characteristics. Finally, the majority of the difference in beta and gamma band power has been determined to be in the striatum as well as parts of the globus pallidus. Direct LFP measurements for these regions are rarer due to not being a target for DBS electrode implantation. This complicates the validation of neuronal dynamics for these regions.

4.2 Inclusion of parallel pathways

In the current experimental design, the inclusion of parallel pathways within the BG has not been used to the fullest degree. Early on, during the adaptation of the model by Goenner et al. parallel pathways were considered due to the various experiments that could be simulated with their inclusion. The relevance of the additional pathways is currently limited to acting as an additional source of noise and possibly delaying the primary reaction. An interesting addition to the Stop Signal task in particular would be to vary the salience of the pathways and measure if it produces a noticeable lag in action selection. Additionally, it might also be interesting to investigate the mechanics of pivoting from one motor programme to another, as opposed to halting all actions. This is a possibility that could be implemented by replacing the Stop signal with another programme of varying salience, basically switching inputs partway through the previous task. In the context of PD, which is known to have difficulties with task switching, this would be an interesting avenue to explore.

4.3 Inclusion of the GPe-subpopulations

The classical model of the BG proposes that overactivity and an increase in connectivity in the STN-GPe loop in PD cause at least a part of the motor symptoms associated with the disease. In light of recent advances, this view has become more nuanced. The finding that the STN responded to both Stop and Go cues as well as newly characterized subsets of neurons in the Globus Pallidus External segment lead Mallet et al. [20] to propose a new scheme of inhibition. It was proposed that these subpopulations of GPe neurons, the Arkypallidal and corticopallidal neurons, reacted specifically to Stop signals. In light of this hypothesis, it seemed relevant to include these subpopulations to the model. These subpopulations produced a different frequency profile compared to the Prototypical GPe neurons. The Arkypallidal GPe neurons had notably higher power in located in the beta band in response to various cortical inputs. The corticopallidal GPe neurons also exhibited the greatest period of significant differences between the control and Parkinsonian condition compare to the other parts of the GPe. These findings seem to justify the subdivision of the GPe in this model as each part exhibits different responses to the experimental signals and were instrumental in the construction of an appropriate output site for the Stop signal.

4.4 Role of the Fast Spiking Interneurons

In a similar vein to the GPe subpopulations, the Fast Spiking Interneurons are, in theory, an important facilitator of striatal inhibition originating in the Globus Pallidus. This function was mostly absent in the current modelling scheme and the population as a whole had little impact on the outcome of the experiments. This can be determined from the dormant state the FSIs were in during almost the entirety of the experiment, leading to no interaction with the

MSNs. Whether the FSIs were incorrectly implemented into the model, or this population is simply not active during inhibition tasks is an important step for further refinement of the model. Although it seems unlikely the population as a whole should be inactive. For future experimental considerations the role of the FSI should be re-examined and if they are found to be relevant, renewed parameter fitting might be fruitful.

4.5 Statistical power of the results

One major hurdle in assessing the results generated by the model is the lack of certainty that can be gained from the results. The sample sizes generated for the experiments are significantly lower when compared to patient studies. The reduced sample size is a consequence of the time constraints imposed on the experiments by the excessive calculation times of the differential equation solver.

Using the GoRTs obtained from the Stop/Signal trials a new power analysis can be performed. The minimum sample size per group for an expected effect of 10 ms with a standard deviation of 18 ms is 17. Given that for every GO trial at least as many successful and unsuccessful Stop trials are need and that there are two conditions for this setup, this yields a total minimum amount of trials of 102. This result does not differ much from the sample size calculated at the start of the trial, which was calculated to be 104 trials. This was under the assumption that the amount of Go- and Stop-trials would be the same however.

4.6 Computational expenses and potential alternatives

The time resolution obtained from the current method of calculation was needlessly fine. The raw simulation results had sampling frequencies approaching 25 kHz, reaching well above any reasonably necessary sampling frequency. While the sheer amount of data facilitated resampling and oversampling for the purposes of frequency analysis, the point still stands that more trials of lesser detail would have been preferable.

A large portion of the hindrances in this model can be traced back to the less than optimal method of calculation of the differential equations. The system of equations was implemented using the Matlab native ddesd functionality. This method allowed for stable simulation as well as relatively easy implementation of delayed interaction between neurons, simulating synaptic delay. A major limiting factor in the computation time of this method was the way it handles time step calculations. This algorithm can be used to solve non-stiff differential equations, which holds up well when a limited number of differential equations are being solved during a single function call. For larger systems of equations this means a single equations experiencing a steep difference in values slows every other equation. Considering the type of phenomenon being simulated, fast spiking neurons, this happens quite often.

A possible solution would be the implementation of another algorithm for solving systems of differential equations. Using a custom Euler method or equivalent with either fixed or controlled time steps could allow one to control the amount of data being calculated during a trial. Alternatively, one could use more specialized software packages to run the simulations. An example of this would the NEURON package for Python or EBRAINS by the Human Brain Project, which also runs on Python. Using either solution would allow for greater control of the computational expenses as well as a greater degree of fine tuning when necessary.

4.7 Future Considerations

Taking into account the hurdles the model has to overcome to truly become viable there are a few interesting directions that could be explored. The use of variable inputs into the parallel pathways might the model to perform action selection tasks, key parameters of interest being reaction speed in relation to conflict complexity. Another experiment that might be interesting is the Go/NoGo task, which is related to the Stop Signal task but relates more to action preparation and precise execution as opposed to inhibition of motor programmes.

The investigation into the pathological effects of Parkinson's Disease could also be studied further. Using the Stop Signal task additional case could be added to the experiment, for various values of the dopamine factor d. This would test the inhibitory efficiency for a gradient of severities, ultimately allowing a relation between this factor and the SSRT to be established. Assuming, that the dopamine factor in the model is a valid method the create a Parkinsonian condition. The implementation of treatment effects modeling the influence of Levadopa or localized DBS stimulation of the STN could also be attempted. The outcome of these simulations could be compared to Stop Signal test experiments, which are plentiful for different treatment methods. This could be an additional venue for model validation.

There are other methods to simulate the pathological state of PD. Increasing the connectivity between the striatal populations could replicate the reported loss of functional segregation. Another possibility would be to tweak the connectivity parameters in the STN-GPe loop, which in previous studies has been demonstrated to induce tremor-like patterns.

There are quite a few possible directions this model could be taken if the computational challenges are overcome and it can be more thoroughly validated as a result.

References

[1] Alegre, M., Lopez-Azcarate, J., Obeso, I., Wilkinson, L., Rodriguez-Oroz, M. C., Valencia, M., Garcia-Garcia, D.,

Guridi, J., Artieda, J., Jahanshahi, M., and Obeso, J. A. The subthalamic nucleus is involved in successful inhibition in the stop-signal task: A local field potential study in parkinson's disease. *Experimental Neurology 239* (1 2013), 1–12.

[2] Claassen, D. O., Wildenberg, W. P. V. D., Harrison, M. B., Wouwe, N. C. V., Kanoff, K., Neimat, J. S., and Wylie, S. A. Proficient motor impulse control in parkinson disease patients with impulsive and compulsive behaviors. *Pharmacology Biochemistry and Behavior 129* (2 2015), 19–25.

[3] Dauer, W., and Przedborski, S. Parkinson's disease: Mechanisms and models. *Neuron 39* (9 2003), 889–909.

[4] Erkkinen, M. G., Kim, M. O., and Geschwind, M. D. Clinical neurology and epidemiology of the major neurodegenerative diseases. *Cold Spring Harbor Perspectives in Biology 10* (4 2018).

[5] Esteban-Peñalba, T., Paz-Alonso, P. M., Navalpotro-Gómez, I., and Rodríguez-Oroz, M. C. Functional correlates of response inhibition in impulse control disorders in parkinson's disease. *NeuroImage: Clinical 32* (1 2021).

[6] Foster, N. N., Barry, J., Korobkova, L., Garcia, L., Gao, L., Becerra, M., Sherafat, Y., Peng, B., Li, X., Choi, J. H., Gou, L., Zingg, B., Azam, S., Lo, D., Khanjani, N., Zhang, B., Stanis, J., Bowman, I., Cotter, K., Cao, C., Yamashita, S., Tugangui, A., Li, A., Jiang, T., Jia, X., Feng, Z., Aquino, S., Mun, H. S., Zhu, M., Santarelli, A., Benavidez, N. L., Song, M., Dan, G., Fayzullina, M., Ustrell, S., Boesen, T., Johnson, D. L., Xu, H., Bienkowski, M. S., Yang, X. W., Gong, H., Levine, M. S., Wickersham, I., Luo, Q., Hahn, J. D., Lim, B. K., Zhang, L. I., Cepeda, C., Hintiryan, H., and Dong, H. W. The mouse cortico–basal ganglia–thalamic network. *Nature 598* (10 2021), 188–194.

[7] Gauggel, S., Rieger, M., and Feghoff, T.-A. Inhibition of ongoing responses in patients with parkinson's disease. *Journal of Neurology, Neurosurgery & Psychiatry 75*, 4 (2004), 539–544.

[8] Goenner, L., Maith, O., Koulouri, I., Baladron, J., and Hamker, F. H. A spiking model of basal ganglia dynamics in stopping behavior supported by arkypallidal neurons. *Eur J Neurosci 53* (2021), 2296–2321.

[9] Gonzalez-Latapi, P., Bayram, E., Litvan, I., and Marras, C. Cognitive impairment in parkinson's disease: Epidemiology, clinical profile, protective and risk factors. *Behavioral Sciences 11* (5 2021).

[10] Gurney, K., Prescott, T. J., and Redgrave, P. A computational model of action selection in the basal ganglia. i. a new functional anatomy. *Biological Cybernetics 84* (2001), 401–410.

[11] Gurney, K., Prescott, T. J., and Redgrave, P. A computational model of action selection in the basal ganglia. ii. analysis and simulation of behaviour. *Biological Cybernetics 2001 84:6 84* (2001), 411–423.

[12] Hashemiyoon, R., Kuhn, J., and Visser-Vandewalle, V. Putting the pieces together in gilles de la tourette syndrome: Exploring the link between clinical observations and the biological basis of dysfunction. *Brain Topography 30* (1 2017), 3–29.

[13] Hauser, R. A. Levodopa: Past, present, and future. *Eur Neurol 62* (2009), 1–8.

[14] Humphries, M. D., Wood, R., and Gurney, K. Dopamine-modulated dynamic cell assemblies generated by the gabaergic striatal microcircuit. *Neural Networks 22* (10 2009), 1174–1188.

[15] Izhikevich, E. M. Simple model of spiking neurons. *IEEE Transactions on Neural Networks 14* (11 2003), 1569–1572.

[16] Izhikevich, E. M. Which model to use for cortical spiking neurons? *IEEE TRANSACTIONS ON NEURAL NETWORKS 15* (2004), 1063.

[17] Jankovic, J. Parkinson's disease: clinical features and diagnosis. *Journal of Neurology, Neurosurgery Psychiatry 79* (4 2008), 368–376. Used in the introduction; relates to the description of the symptoms of PD, in particular the cardinal symptoms.

[18] Kim, H. F., and Hikosaka, O. Parallel basal ganglia circuits for voluntary and automatic behaviour to reach rewards. *Brain 138* (7 2015), 1776–1800.

[19] Logan, G. D., Cowan, W. B., and Davis, K. A. On the ability to inhibit simple and choice reaction time responses: A model and a method. *Journal of Experimental Psychology: Human Perception and Performance 10* (4 1984), 276–291.

[20] Mallet, N., Schmidt, R., Leventhal, D., Chen, F., Amer, N., Boraud, T., and Berke, J. D. Arkypallidal cells send a stop signal to striatum. *Neuron 89* (2016), 308–316.

[21] Manza, P., Amandola, M., Tatineni, V., Li, C. S. R., and Leung, H. C. Response inhibition in parkinson's disease: A meta-analysis of dopaminergic medication and disease duration effects. *npj Parkinson's Disease 3* (2017).

[22] Mehanna, R., and Lai, E. C. Deep brain stimulation in parkinson's disease, 2013.

[23] Nagao, K. J., and Patel, N. J. From medications to surgery: Advances in the treatment of motor complications in parkinson's disease. *Drugs in Context 8* (2019).

[24] Nambu, A., Tokuno, H., and Takada, M. Functional significance of the cortico–subthalamo–pallidal 'hyperdirect' pathway. *Neuroscience Research 43* (6 2002), 111–117.

[25] Navarro-López, E. M., Çelikok, U., and Şengör, N. S. A dynamical model for the basal ganglia-thalamo-cortical oscillatory activity and its implications in parkinson's disease. *Cognitive Neurodynamics 15* (8 2021), 693–720.

[26] Neumann, W. J., Staub-Bartelt, F., Horn, A., Schanda, J., Schneider, G. H., Brown, P., and Kühn, A. A. Long term correlation of subthalamic beta band activity with motor impairment in patients with parkinson's disease. *Clinical Neurophysiology 128* (11 2017), 2286–2291.

[27] Pani, P., Bello, F. D., Brunamonti, E., D'Andrea, V., Papazachariadis, O., and Ferraina, S. Alpha- and beta-band oscillations subserve different processes in reactive control of limb movements. *Frontiers in Behavioral Neuroscience 8* (11 2014).

[28] Parasuram, H., Nair, B., D'Angelo, E., Hines, M., Naldi, G., and Diwakar, S. Computational modeling of single neuron extracellular electric potentials and network local field potentials using lfpsim. *Frontiers in Computational Neuroscience 10* (6 2016).

[29] Ray, N. J., Brittain, J. S., Holland, P., Joundi, R. A., Stein, J. F., Aziz, T. Z., and Jenkinson, N. The role of the subthalamic nucleus in response inhibition: Evidence from local field potential recordings in the human subthalamic nucleus. *NeuroImage 60* (3 2012), 271–278.

[30] Ray, N. J., Jenkinson, N., Brittain, J., Holland, P., Joint, C., Nandi, D., Bain, P. G., Yousif, N., Green, A., Stein, J. S., and Aziz, T. Z. The role of the subthalamic nucleus in response inhibition: Evidence from deep brain stimulation for parkinson's disease. *Neuropsychologia 47* (11 2009), 2828–2834.

[31] Rubin, J. E., and Terman, D. High frequency stimulation of the subthalamic nucleus eliminates pathological thalamic rhythmicity in a computational model. *Journal of Computational Neuroscience 16* (2004), 211–235.

[32] Schmidt, R., and Berke, J. D. A pause-then-cancel model of stopping: Evidence from basal ganglia neurophysiology. *Philosophical Transactions of the Royal Society B: Biological Sciences 372* (4 2017).

[33] Simonyan, K. Recent advances in understanding the role of the basal ganglia [version 1; referees: 2 approved]. *F1000Research 8* (2019).

[34] Surmeier, D. J., Ding, J., Day, M., Wang, Z., and Shen, W. D1 and d2 dopamine-receptor modulation of striatal glutamatergic signaling in striatal medium spiny neurons. *Trends in neurosciences 30* (5 2007), 228–235. Used in the introduction; provides description of the dopamine receptors in the striatum.

[35] Tan, E. K. Dopamine agonists and their role in parkinson's disease treatment. *http://dx.doi.org.ezproxy2.utwente.nl/10.1586/14737175.3.6.805 3* (11 2014), 805–810.

[36] Thibeault, C. M., and Srinivasa, N. Using a hybrid neuron in physiologically inspired models of the basal ganglia. *Frontiers in Computational Neuroscience 7* (6 2013), 88.

[37] van den Wildenberg, W. P., Ridderinkhof, K. R., van Wouwe, N. C., Neimat, J. S., Bashore, T. R., and Wylie, S. A. Overriding actions in parkinson's disease: Impaired stopping and changing of motor responses. *Behavioral Neuroscience 131* (10 2017), 372–384.

[38] Verbruggen, F., and Logan, G. D. Models of response inhibition in the stop-signal and stop-change paradigms. *Neuroscience Biobehavioral Reviews 33* (5 2009), 647–661.

[39] Wang, C. H., Chang, C. C., Liang, Y. M., Shih, C. M., Chiu, W. S., Tseng, P., Hung, D. L., Tzeng, O. J., Muggleton, N. G., and Juan, C. H. Open vs. closed skill sports and the modulation of inhibitory control. *PLoS ONE 8* (2 2013).

[40] Wenning, G. K., Litvan, I., and Tolosa, E. Milestones in atypical and secondary parkinsonisms.

[41] Wessel, J. R., Ghahremani, A., Udupa, K., Saha, U., Kalia, S. K., Hodaie, M., Lozano, A. M., Aron, A. R., and Chen, R. Stop-related subthalamic beta activity indexes global motor suppression in parkinson's disease. *Movement Disorders 31* (12 2016), 1846–1853.

[42] Ye, Z., Altena, E., Nombela, C., Housden, C. R., Maxwell, H., Rittman, T., Huddleston, C., Rae, C. L., Regenthal, R., Sahakian, B. J., Barker, R. A., Robbins, T. W., and Rowe, J. B. Improving response inhibition in parkinson's disease with atomoxetine. *Biological Psychiatry 77* (2015), 740–748. Highlighted segments show significantly longer SSRTs in PD.